

Topical Review

Review of polymer MEMS micromachining

Brian J Kim and Ellis Meng

Department of Biomedical Engineering, University of Southern California, 1042 Downey Way, DRB-140, Los Angeles, CA 90089-1111, USA

E-mail: ellis.meng@usc.edu

Received 5 February 2015, revised 11 October 2015

Accepted for publication 15 October 2015

Published 19 November 2015



CrossMark

Abstract

The development of polymer micromachining technologies that complement traditional silicon approaches has enabled the broadening of microelectromechanical systems (MEMS) applications. Polymeric materials feature a diverse set of properties not present in traditional microfabrication materials. The investigation and development of these materials have opened the door to alternative and potentially more cost effective manufacturing options to produce highly flexible structures and substrates with tailorable bulk and surface properties. As a broad review of the progress of polymers within MEMS, major and recent developments in polymer micromachining are presented here, including deposition, removal, and release techniques for three widely used MEMS polymer materials, namely SU-8, polyimide, and Parylene C. The application of these techniques to create devices having flexible substrates and novel polymer structural elements for biomedical MEMS (bioMEMS) is also reviewed.

Keywords: polymer, mems, micromachining, etching

(Some figures may appear in colour only in the online journal)

1. Introduction

Polymer-based technologies introduced in the 1990s have played a large role in advancing MEMS into new applications, especially in the area of biomedical MEMS (or bioMEMS). Micromachined polymers may be employed as structural or functional elements as well as soft, flexible substrates that contain other devices. This versatility is afforded by the development of a wide range of processing techniques unique to polymer materials. For example, simple polymer structural elements can be photopatterned or casted, eliminating the need for complicated etching steps and lithographic masking required in silicon processing. A major advantage of such processing approaches is the reduction in cost to manufacture micro and nano structures.

The properties of polymers also play an important role in driving new applications as well as device performance. Low Young's modulus polymer films permit delicate, non-destructive interactions with pliable cells and tissues, creating a mechanically favorable environment within these biological systems; the bulk mechanical properties are often tunable over

a wide range. Many polymers also exhibit chemical and biological inertness desired in *in vitro* (e.g. lab-on-a-chip (LOC)) or *in vivo* (e.g. implant) applications. Furthermore, polymer surfaces are readily functionalized to modify surface properties to desired specifications.

Many polymers have been explored in the research literature for MEMS applications: including SU-8, polyimide, Parylene, polydimethylsiloxane (PDMS), liquid crystal polymers (LCPs), cyclic olefin polymers (COPs), polymethyl methacrylate (PMMA or plexiglass), polycarbonate (PC), and polystyrene (PS). It is the combination of material properties, processing conditions, and performance demands that drives selection of a particular polymer for a device. PDMS is one of the most widely used polymers largely due to low cost and low infrastructure needs of soft lithography techniques that enable simple construction of micro and nano features [1]. The use of PDMS to construct microfluidic devices by casting pre-polymer onto a rigid mold has found widespread adoption among the research community [2]. LCPs possess unique mechanical properties by virtue of their structure, in which rigid and flexible monomers are linked to each other

with a strategic alignment of rigid segments to specific directions. LCPs exhibit improved barrier properties and adhesion and are being explored as a potential replacement material for polyimides [3]. COPs have gained popularity as a material for microfluidics for their high chemical and biological inertness and low water absorption [4]. PMMA, PC, and PS are thermoplastic polymers typically used for microfluidic applications, and have found success with hot embossing techniques to form devices largely due to their mechanical strength with relatively low glass transition temperature (T_g), low-cost, and biocompatibility [5].

Among the polymers mentioned above, SU-8, polyimide, and Parylene are currently on the rise within MEMS as free-film substrates and structural elements on hybrid silicon-polymer devices. Compared to the other polymers, these three are compatible with more standard microfabrication techniques, i.e. photolithography and wet/dry etches, which have motivated a large effort within the community to develop novel strategies for processing and device construction. As a summary of these efforts, this review presents a high-level overview of often used and recently developed processing techniques and a brief description of notable devices for these three polymers. A brief, high level overview of the details of this review is presented in table 1. For additional information, the reader is also referred to [6–10] for supplementary reviews of polymers within MEMS.

2. SU-8

The use of photolithography for direct creation of structural materials for MEMS has led to the development of photoresists that can be processed as thicker layers ($>5 \mu\text{m}$). Of these, the most widely used is SU-8, developed and later patented by IBM in 1989 (US patent 4882245) [142]. SU-8 has served as a popular low cost alternative to create relatively thick structures with high aspect ratios without having to resort to x-ray lithography or deep reactive ion etching. The first reported use of SU-8 in MEMS was in 1997 as a replacement for x-ray lithography in LIGA processes, a process later known as ‘UV-LIGA’ or ‘poor man’s LIGA.’ SU-8 was later commercialized by MicroChem Corporation (Westborough, MA), Gersteltec (Pully, Switzerland), and DJ DevCorp (Sudbury, MA), with each vendor creating specialized formulations of the material: e.g. SU-8 2000 from MicroChem, formulated with a cyclopentanone solvent, has shown to have excellent coating and adhesion properties and DJ DevCorp’s SUEX™ is produced as a dry film sheet for lamination.

SU-8’s chemically amplified resist formulation was developed to achieve high aspect ratios and thick layers [143]. Commercial SU-8 formulations typically consist of a bisphenol-A novolac resin with 8 epoxy groups [11] (EPON SU-8 resin, a registered trademark of Shell chemical company), a solvent (e.g. cyclopentanone or GBL, gamma-butyrolactone), and up to 5–10% in weight of a photoacid initiator [22, 144], usually triarylsulfonium hexafluoroantimonate [9, 142, 145]. The exposure of this polymer to UV light generates a strong photoacid, which protonates the epoxy groups of the monomer

and starts a cross-linking reaction to create a highly cross-linked polymer [146].

Typically, lithography of SU-8 involves a set of processing steps similar to standard thick photoresists: (1) deposition on a substrate (usually via spinning), (2) a softbake to evaporate the solvent, (3) exposure to cross-link the polymer, (4) post-exposure bake to finalize the cross-linking, and (5) development to reveal the cross-linked structure. SU-8 developers include methyl isobutyl ketone (MIBK) and propylene glycol methyl ether acetate (PGMEA) [11]. Following exposure, the uncrosslinked resist is typically developed in PGMEA, but immersion first in gamma butyrolactone (GBL) can improve development for high aspect ratio (HAR) channels. Typically, thick films of a few hundred microns can be constructed with conventional UV exposure systems which is attributed to SU-8’s (1) low molecular weight [11] and (2) low absorbance in the near-UV spectrum ($\sim 46\%$ at 365 nm) [144]. This negative tone, epoxy type resist has many favorable properties and is widely used for its versatility as a MEMS material. For a more thorough review of SU-8, the authors refer the reader to [11, 146–150].

2.1. Properties summary

SU-8’s aromatic structure and high degree of cross-linking results in its high thermal and chemical stability. Consequently, SU-8 is also proton radiation tolerant [151]. SU-8 has been employed in a wide range of devices for its tunable electrical [12, 13], magnetic [14], optical [15, 16], and mechanical properties [17–19]. However, SU-8 properties can vary widely depending on the processing conditions [51].

Patterned SU-8 structures are popular as molds for soft lithography and the construction of silicone-based LOC/microfluidic devices due to its chemically stable and mechanically robust structure. In addition, SU-8 has a high refractive index and low loss over a wide wavelength range, making the material ideal for fabricating optical waveguides [20, 21]. Specifically for *in vivo* and *in vitro* applications, SU-8 has been reported to have decent chemical and biocompatibility [145, 152, 153], but still has not attained the USP Class VI material rating for biocompatibility; studies have shown that SU-8 is associated with antimony-based leachates from the photoacid of the material, which can compromise its potential cellular or biological compatibility [145].

2.2. Micromachining strategies

2.2.1. Photopatterning techniques. One processing advantage of SU-8 compared to other MEMS polymers is the simplicity of creating thick films and structures over a large range of thicknesses. SU-8 films can be spun to $>500 \mu\text{m}$ thick in a single layer and multiple spins can achieve 1.2 mm thick films with an aspect ratio of 18 [22]. For these thick spins, SU-8 can self-planarize and reflow to reduce edge bead build-up during the soft bake step [22].

With SU-8, it is also possible to utilize multiple exposure steps on multiple layers that are subsequently released in a

Table 1. High-level overview of polymers within this review.

Polymer	Properties summary	Fabrication overview	Examples of applications	Fabrication challenges
SU-8	<ul style="list-style-type: none"> • High thermal and chemical stability [11] • Tunable properties [12–19] • Low optical loss [20, 21] 	<ul style="list-style-type: none"> • Thick photopatternable films [22] • Multiple exposure steps and single development [23–26] • Backside exposure [27, 28] • SU-8 to polymer bonding [29, 30] • Etching is difficult and rates are slow [31]; mechanical processes necessary [32, 33] 	<ul style="list-style-type: none"> • Structural molds for soft lithography [34] • Microfluidics [35, 36] • Microneedles [37, 38] • Optical waveguides [27, 39, 40] • Neural probes [39, 41] 	<ul style="list-style-type: none"> • Properties of film dependent on processing parameters [42, 43] • Importance of exposure on dimensional accuracy and resolution [33, 43–53] • Large stresses between SU-8 and substrate [54–56]
Polyimide	<ul style="list-style-type: none"> • High thermal and chemical stability [57–59] • Low moisture absorption [58] • Tailorable film via chemical modification [60, 61] • Photosensitized formulations [62] • Biocompatible [63–65] 	<ul style="list-style-type: none"> • Pattern photosensitive polyimides [60, 66] • Dry etching of using oxygen or fluorine chemistries [67–73] • Hot embossing capability [74, 75] • Surface modification using plasma [76] 	<ul style="list-style-type: none"> • Flexible microelectrode arrays [63, 65, 71, 77–86] • Sensors [87–89] • Microchannels [90] • Lab-on-a-tube technology [91, 92] • Self-assembly via imidization shrinkage [93, 94] 	<ul style="list-style-type: none"> • Poor adhesion onto materials [95] • Significant shrinkage during imidization process [79, 95, 96]
Parylene C	<ul style="list-style-type: none"> • Chemical inertness [97, 98] • Uniform and conformal CVD • Gas phase, pinhole-free deposition • Low intrinsic stress [99] • High transmittance in visible spectrum [100–104] • Biocompatible [105–107] 	<ul style="list-style-type: none"> • Deposition onto structured surfaces and liquids [108–111] • Dry etching of using oxygen or fluorine chemistries [112–115] • Hot embossing and thermal forming [116–119] • Surface modification using plasma [120, 121] 	<ul style="list-style-type: none"> • Microchannels [122–125] • Sensors [126–129] • Neural probes [130, 131] • Cuff electrodes [132, 133] • Retinal and cochlear implants [108, 134, 136] 	<ul style="list-style-type: none"> • Sensitive to temperature (low T_g) [122] • Adhesion issues between Parylene-Parylene and Parylene-metal in soaking conditions [137–141]

single development [23–26]. For this method, the first SU-8 layer is spun on and exposed. Then, instead of developing, a second layer of SU-8 is spun on and exposed. SU-8 layers are repeatedly applied and exposed until the final layer of the device is processed. In the final step, all unexposed regions would be developed away in a single development step, greatly simplifying the fabrication process (figure 1(a) and 2(a)) [154, 155]. However, when using this technique, the dimensions of each subsequent overlying layer must be smaller than or the same as that of the adjacent lower layer to prevent the exposure of the lower layer. One method around this limitation is to use a diluted SU-8 resist with a lower concentration of photoacid initiator for the lower layer so as to create a resist that is less sensitive and has lower absorption to UV; this base layer would then be less susceptible to unwanted exposure during exposures of the overlying layers [155]. Along similar lines, rounded SU-8 structures can also be constructed by using the time-based diffusion of the photoacid initiator into the overlying layer following exposure of the underlying layer [156].

Unconventional UV exposure methods can be used to form structures that are difficult to obtain using standard MEMS materials. For example, to create protective sealing caps at the

wafer-level, partial exposure (i.e. underexposure) of SU-8 was used to crosslink the top of a cap, while the region underneath was not exposed (figure 1(b)) [157]. Unexposed SU-8 was developed away through access ports patterned on the lid. A final lithographic step then sealed the holes and package. This underexposure technique was applied to also form the base structure for a microneedle array by controlling the depth of exposure [38]. Correspondingly, SU-8 is also compatible with grey scale lithography, i.e. exposure variation over the SU-8 using a grey scale photomask, to form multi-level structures in a single exposure [158].

To avoid issues of high fidelity pattern transfer in thicker films, backside exposure, i.e. exposing through the backside of a UV transparent wafer, has been proposed. To pattern thick, high aspect ratio (HAR) structures, intimate contact between the resist and the mask is required for optimal pattern transfer; thus, a hard contact or vacuum contact mode is used during exposure. Small deviations in the planarity at the top of the thick resist introduce diffraction errors during exposure which increase linearly with the gap between the mask and the photoresist [159]. UV transparent substrates (e.g. glass, quartz, and sapphire) exist that are flat and can incorporate opaque masking

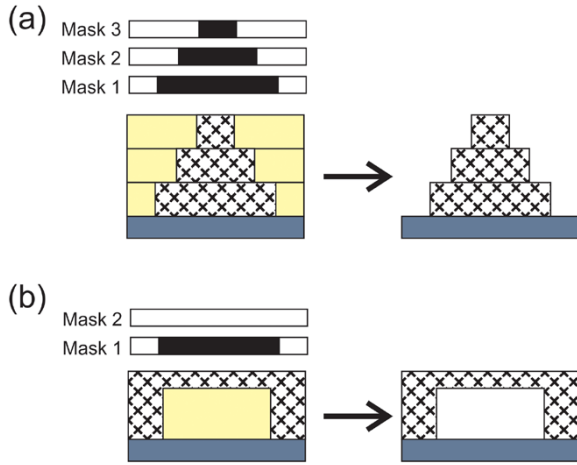


Figure 1. (a) Schematic of multiple exposure steps of SU-8, where a layer of SU-8 is spun on and then exposed with Mask 1. Then a second layer of SU-8 is spun on and exposed with Mask 2, and a last layer of SU-8 is spun on and exposed with Mask 3. Following development the pyramid structure is released. (b) Schematic of forming a cap on SU-8 posts using two masks: Mask 1 is used to expose a thick SU-8 layer to create the posts and Mask 2 is used to underexpose the top surface of the layer to form the cap.

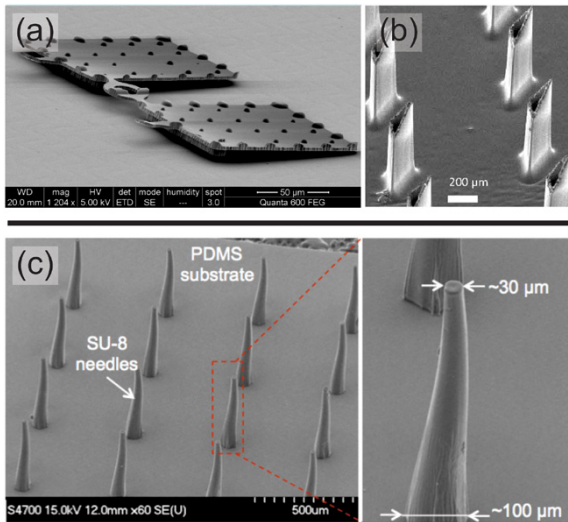


Figure 2. (a) SEM image of fully released scratch drive microrobot fabricated using a single development step to produce a multi-layer/ exposed SU-8 structure. © 2011 IEEE. Reprinted, with permission, from Valencia M *et al* 2011 Development of untethered SU8 polymer scratch drive microrobots 2011 *IEEE 24th Int. Conf. on Micro Electro Mechanical Systems* pp 1221–4 [154]. (b) SEM image of beveled SU-8 microneedles formed using an inverted exposure technique with tapered molds etched into the Si substrate. © 2013 IEEE. Reprinted, with permission, from Chaudhuri B P *et al* 2013 A novel method for monolithic fabrication of polymer microneedles on a platform for transdermal drug delivery 35th *Annual Int. Conf. of the IEEE Engineering in Medicine and Biology Society* pp 156–9 [37]. (c) SEM images of implantable SU-8 waveguides for optogenetics patterned using backside exposure technique. © 2013 IEEE. Reprinted, with permission, from Kwon K and Li W 2013 Integrated multiLED array with three-dimensional polymer waveguide for optogenetics 2013 *IEEE 26th Int. Conf. on Micro Electro Mechanical Systems* pp 1017–20 [39].

features, usually through a thin film metal layer. The bottom layer of the resist maintains intimate contact with the substrate and mask, allowing HAR structures to be faithfully produced. This technique has also been used to form inclined structures by tilting the wafer/SU-8 assembly with respect to the exposure source [27] and tapered structures by leveraging refractive index differences produced by etched features in the substrate (such as an isotropically etched glass to form an ‘integrated lens’ [28]). A similar idea was also used to form tapered and multi depth structures using backside exposure of a droplet of SU-8 [41]. For a more thorough review on the backside exposure technique for SU-8, the reader is referred to [28].

SU-8 can be also applied onto pre-structured substrates, such as etched silicon [37] or PDMS [38] structures to form microneedles. This technique can be used to achieve double-sided micro structuring of SU-8 [53]. Mold materials should be selected based on the criteria of thermal compatibility (i.e. thermal budget) during SU-8 processing (e.g. softbake, post-exposure bake) to ensure dimensional accuracy [38]. It is important to note that nonplanar mold structures may result in unwanted reflections/refractions during exposure that can lead to additional dimension inaccuracies and unwanted exposure. This can be mitigated by controlling the angle of these structures as guided by Snell’s law and Fresnel’s equations [38], or via the use of antireflection coatings or layers that can absorb incident UV irradiation [160, 161]. For molds with significantly uneven surfaces where spinning is insufficient to achieve the desired planarity, SU-8 can also be applied by spray coating [162], powder casting [163], or by lamination when using dry-film SU-8 [55].

In addition to large area UV exposure, SU-8 is amenable to direct writing via both excimer [164, 165] and femtosecond (via two-photon-absorption patterning) [166] laser, e-beam [167], and proton beam [168–170] to expose small complex features. This technique can be further tuned by using in-focus and out-of-focus methods to control the exposure area; the out-of-focus technique can expose a thin superficial layer of SU-8 [165]. In addition, the combination of standard UV lithography with stereolithography of SU-8 allows for the fabrication of complex 3D structures. High aspect ratio structures in SU-8 have been achieved through x-ray lithography (LIGA) [171] and deep proton writing [172].

2.2.2. Removal techniques. The cross-linked nature of SU-8 imparts chemical stability, which in turn makes removal of cured SU-8 difficult. Practical removal requires mechanical techniques (e.g. crazing, peeling, or cracking) or strong chemistries. Typical wet etch recipes for SU-8 include hot 1-methyl-2-pyrrolidone (NMP), piranha etch (H_2SO_4 , H_2SO_4/H_2O_2), and fuming HNO_3 [147, 173]. Commercial SU-8 strippers are also available, including NANO™ RemoverPG, ACT-1, QZ3322, MS-111, Magnastrip, RS-120, and K10 molten salt bath. Ozone solution can also remove SU-8 [174], but removal rates are slow; the rate can be improved by using ozone steam [175]. However the ozone solution, as well as other stronger solutions, may not be compatible with other materials present in a device; nickel corrosion was reported after exposure to ozone [175].

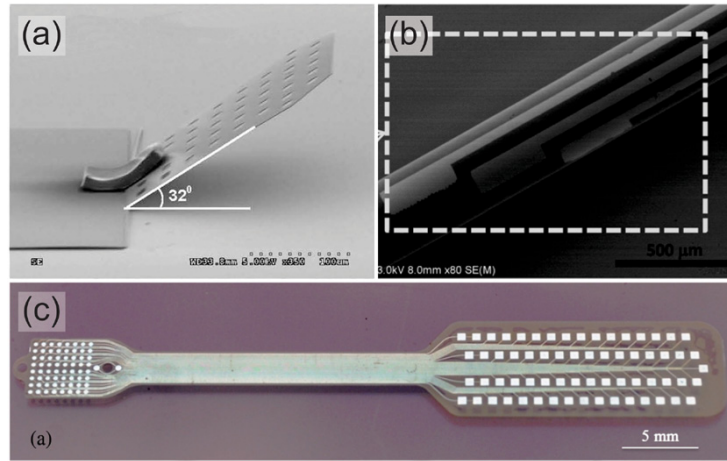


Figure 3. (a) SEM image of polyimide-hinge, self-assembled polysilicon microplate leveraging the shrinkage of polyimide during imidization. Reproduced with permission from Huang I-Y *et al* 2010 Lifting angle of polyimide self-assembly surface-micromachined structure *J. Micro Nanolith. MEMS MOEMS* 9 023006 [286], © 2010 Society of Photo-Optical Instrumentation Engineers. (b) SEM image of ‘lab-on-a-tube’ technology device with microelectrodes patterned onto a 3D cylindrical polyimide tube. Reproduced from [92] with permission of The Royal Society of Chemistry. (c) Image of dual-metal layer thin-film polyimide 64 channel implantable microelectrode array for retinal stimulation [65]. Reproduced from Jiang X *et al* 2013 *In vitro* and *in vivo* evaluation of a photosensitive polyimide thin-film microelectrode array suitable for epiretinal stimulation *J. NeuroEng. Rehabil.* 10 48, with permission from BioMed Central.

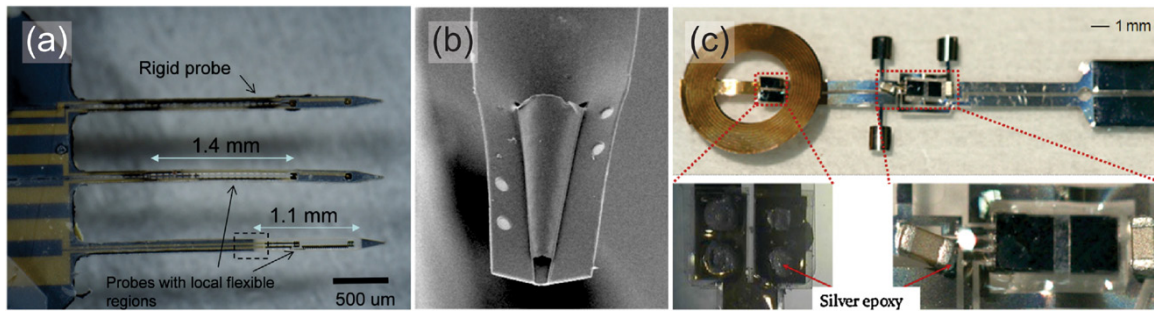


Figure 4. (a) Optical micrograph of hybrid Parylene-silicon neural probe with local flexible regions. Reprinted from Kim E G *et al* 2014 A hybrid silicon-parylene neural probe with locally flexible regions *Sensors Actuators B* 195 416–22, copyright 2014, [341], with permission from Elsevier. (b) Thermally formed implantable Parylene sheath electrode with Parylene 3D conical structure encapsulating electrodes. © 2013 IOP Publishing. Reproduced by permission of IOP Publishing from [130]. All rights reserved. (c) All-inclusive packaged retinal stimulator with discrete electronics and coil on a single Parylene substrate. Reprinted from Li W *et al* 2011 Parylene-based integrated wireless single-channel neurostimulator *Sensors Actuators A* 166 193–200, copyright 2011, [135], with permission from Elsevier.

Physical methods such as water jetting [32], pyrolysis [33], and excimer laser patterning [176] can also be used to remove SU-8. The latter method results in nanoscale roughness because of redeposited debris, which can create superhydrophobic surfaces [176]. These aggressive physical techniques can cause damage to the underlying substrate, and are not recommended for precise removal of SU-8 for small features.

Dry etching of SU-8 is also possible, but with slow etch rates [31]. Removal in oxygen (O_2) and O_2 /fluorine (e.g. CF_4 , SF_6) plasmas has been reported (etch rates of $0.9 \mu m \text{ min}^{-1}$ for O_2 , $1.27 \mu m \text{ min}^{-1}$ for O_2/CF_4 , and $1.5\text{--}2 \mu m \text{ min}^{-1}$ for O_2/SF_6 [31]). However, these etches have been shown to leave residues (e.g. antimony) on surfaces which originate from the photoacid initiator in SU-8 [174]. One effort has looked into using CHF_3 plasma reactive ion etching, but was only able to achieve etch rates of $0.12 \mu m \text{ min}^{-1}$ [177].

2.2.3. Release techniques. SU-8 films can be separated from the substrate to create free-film devices. The typical approach is to use release layers consisting of metal films such as aluminum (Al) [22, 54, 90], titanium (Ti) [178], copper (Cu) [179, 180], chromium (Cr) [54, 181], or chromium/gold/chromium (Cr/Au/Cr) [182] that are later removed by wet etching [56]. A sacrificial layer of gold by itself cannot be used as SU-8 has been found to have poor adhesion to gold [183]. SU-8 can be released from silicon substrates directly [181, 184, 185]. However, when using potassium hydroxide (KOH) to etch silicon to free the final SU-8 device, the heat required to achieve a reasonable etch rate can introduce added internal stresses within the SU-8, which can lead to micro-cracks or warpage [56].

The use of polymer release layers has also been explored. Groups have looked into the use of photoresists such as AZ

4620 [56], which has the benefit of also being removed during the development of the SU-8 structure. Alternatively, poly methylglutarimide (PMGI) resist can be substituted for AZ resists when the release is required to occur after and not simultaneously with SU-8 development [154]. Polystyrene release layers were employed for release of large area devices (50 cm^2) [186]. Surface assembled monomers (SAMs) can also be used to act as a ‘nanocarpet’ to reduce the adhesion between the substrate and the SU-8 structure for release without the need for chemical removal of the sacrificial layer [187]. A commercial sacrificial layer from MicroChem (Omnicoat™) is also widely used; Omnicoat™ is usually spun prior to spinning SU-8 and is removed using a developer.

SU-8 films can also be released by direct mechanical peeling when adhesion to the underlying material is poor; this avoids the lengthy exposure to chemical etches that may in turn affect SU-8 structures. Candidates include teflon [188, 189], PDMS [190], PET [55], Kapton [191], Pyrex [16], and polyimide [192], but transparent films, such as PDMS and PET, provide the added benefit of facilitating alignment to underlying structures and for backside exposure [190]. Mechanical peeling of SU-8 films from Parylene C was utilized to produce physical masks for metal lift-off [193]. Peeling of SU-8 from a substrate was found to be dependent on its post-exposure baking temperature [194]; SU-8 adhesion to silicon substrates was found to fail for post-exposure bakes $<100\text{ }^\circ\text{C}$, a phenomenon attributed to a lack of hydrogen bonding [195].

2.2.4. Bonding techniques. Construction of capped devices can be achieved by bonding SU-8 interfaces via thermocompression (i.e. application of heat and pressure) through custom or commercial wafer/die bonding systems. This process can enclose microchannels or be used with standard wafer and die-level device bonding, and is accomplished with SU-8 films following spin coating [30, 196], during the soft-bake step [25], or even after the crosslink step [197]. Dry SU-8 film can also be applied via lamination. Bonding of SU-8 to other polymers such as PDMS [29] has also been demonstrated, aided by O_2 plasma treatment to first render the SU-8 surface hydrophilic followed by a chemical modification step (e.g. addition of silane solution, 3-aminopropyltriethoxysilane (APTES)) [29]. Multilayer SU-8 devices have been demonstrated using the BETTS (Bonding, Exposing, Transferring Technique) process, where SU-8 on a release layer substrate is flipped onto a cross-linked SU-8 surface, exposed, and subjected to a post-exposure bake to bond the two parts [30].

2.2.5. Surface and bulk modification. Untreated SU-8 is relatively hydrophobic with a low surface energy (contact angle = $80\text{--}85^\circ$), which may present difficulties in applications such as microfluidics and bioMEMS. Surface treatment can be effective in rendering surfaces hydrophilic. Beyond wet chemical treatment (e.g. ethanolamine [199]), O_2 plasma has been used to improve the hydrophilicity of SU-8 surfaces by generating carbonyl and carboxyl groups on the surface [198]. Although O_2 plasma treatment also increases surface roughness (e.g. from 0.25 to 4 nm mean surface roughness which

varies with process parameters) [198, 200], treated surfaces can maintain hydrophilicity for several weeks [198]. In cases where O_2 plasma treatment is unsuitable, e.g. O_2 induced oxidation to metal seed layers used for electroforming, argon (Ar) plasma may be a suitable alternative. However, increased surface roughness for treatment times up to 30s also results [201]. If surface roughening is undesired, surface functionalization with different polymers may suffice—one group explored the grafting of a photoactivated linker poly ethyleneimine-graft-perfluoro-phenyl azide (PEI-g-PFPA) to covalently bind polymers to the SU-8 interface [202].

Improving hydrophilicity with O_2 plasma treatment facilitates fluid filling in SU-8-based microfluidics [203] and can also promote the attachment of proteins [20, 204] or other biocompatible polymers, e.g. poly ethylene glycol (PEG). These polymers can also be combined with SU-8 either through grafting-based approaches [205] or a unique swelling/deswelling approach, where toluene is used to swell a SU-8 3D lattice structure to capture the polymer segments within the lattice, and is later evaporated out to trap them [206]. However, it is important to note that the plasma treatment of SU-8 can lead to an increase of antimony oxide from the photoacid initiator on the surface, which may adversely interact with cells and tissue [198]—therefore, it is important to clean or otherwise treat the exposed SU-8 surfaces following O_2 plasma.

In contrast to surface modification, pyrolysis can be used to convert bulk SU-8 films into pure carbon structures. Complete carbonization was reported for SU-8 films processed at $900\text{ }^\circ\text{C}$ in an inert atmosphere [146]. The carbonization process leads to the formation of films/structures having a large electrochemically stable window with better geometries than carbon inks or pastes. These films can also be a source for the production of conductive carbon fibers [207]. This technique was employed to create discrete electrical components, including capacitors, batteries, and sensors [146]. A review of this topic is presented in [146].

2.2.6. Fabrication challenges. Several SU-8 processing challenges have been well-documented in the literature [33, 43–53]. Properties of the film are highly dependent on the processing parameters (i.e. soft bake, exposure dosage, and post-exposure bake) [42, 43], and these parameters are important in attaining crack-free films and maintaining dimensional accuracy in structures [52]. For example, SU-8 films are susceptible to a ‘T-topping’ phenomenon where the sidewall profile has a T-shape from the higher absorption of shorter wavelengths, usually exacerbated by the use of broadband UV sources for exposure. Because of this undesired sidewall profile, the optimization of exposure dose [53] and the use of a filtered light source to remove wavelengths below 350 nm [208] have been explored to achieve a straighter sidewall profile. Ultra deep x-ray lithography has also been leveraged to create straight sidewalls and extremely high aspect ratio structures [209].

Diffraction and reflection between the SU-8 and the substrate, mask, and/or wafer chuck during exposure can lead to undesired exposure, which can compromise dimensional accuracy and resolution [37, 161, 194]. One approach to

remedy this is the application of an antireflective coating such as a photoresist layer [160, 161] that can absorb the incident light. Al has also been used [161], but with limited success largely due to its rough surface.

Large stresses can also arise between the SU-8 layer and the substrate. These issues have largely been attributed to the high density crosslinking and large coefficient of thermal expansion (CTE) differences between SU-8 and substrate that can lead to significant shape distortion (e.g. shrinkage, wafer bowing), fracture, and device failure [54–56]. This type of film failure can also occur during plasma etching when SU-8 is used as an etch mask; long etch times (i.e. prolonged wafer heating) can lead to delamination of SU-8 from the substrate layer [210]. Several techniques can prevent thermally induced stresses including the use of ramped softbakes [43, 211, 212], lowering the soft and post exposure bake temperatures [43, 52], and adding a cooling or relaxation step following the post exposure bake [47, 53]. Rest steps during the UV exposure step have also been utilized to avoid thermal stress [165]. Other approaches involve the use of stress adaptive layers for CTE matching (e.g. PET [55], PMMA, polyetheretherketone (PEEK) [213], metals [45, 214], and Parylene C [27]) between the SU-8 and substrate layers. However for these devices, it is important to consider the adhesion of SU-8 on the CTE matching layers [54, 147].

2.3. Notable applications

The simplicity of fabrication has made SU-8 a popular choice in producing inexpensive molds for soft lithography [34] or structural devices for MEMS applications. SU-8 has been used to construct microfluidic channels for LOC devices [35, 36], as well as waveguides, mirrors, and cladding for optical applications [27, 39, 40]. SU-8 has also been the chosen substrate to construct microneedles for drug delivery devices (figure 2(b)) [37, 38], or as waveguides and substrates for cortical implants (figure 2(c)) [39, 41]. SU-8 has also been utilized to form the structures for inclined mirrors for optogenetics applications [27].

In addition to serving as a structural layer, SU-8 has also been investigated as a substrate for free-film devices. SU-8's flexibility was leveraged in the fabrication of insect wings in the development of micro air vehicles (MAVs) [215]. In contrast, its structural stiffness and low water penetration compared to other polymers were the driving reasons for its selection as an enclosure material for implantable pressure sensors [211]. Mechanical and moisture barrier properties also led to the development of flexible neural probes with an integrated microfluidic channel for drug delivery using SU-8 as the structural and substrate material [210]. SU-8 has also been explored as a material to produce self-assembling capsules for drug delivery applications [216].

3. Polyimide

Polyimides have a long rich history dating back to 1908 when the first aromatic forms were synthesized, but were not commercialized until the 1960's and then only in film form

by DuPont [58]. Now, polyimides are available in bulk (as film or tapes backed with pressure-sensitive adhesive) or can be spun on as thin films in both photopatternable and non-photopatternable versions. This versatile class of polymers can be linear (aliphatic) or cyclic (aromatic) in structure and the cured material can exhibit both thermoset or thermoplastic behavior [58]. Synthesis generally starts with a polyamic acid precursor that is imidized at elevated temperatures (typically 300–500 °C) in a nitrogen environment to form the final polyimide structure [217]. The imidization process involves solvent removal and subsequent ring closure in aromatic versions [218]. The polyamic acid precursor is soluble in polar inorganic solvents including *n*-methylpyrrolidone (NMP), dimethyl formamide (DMF), and dimethylsulfoxide (DMSO) [218].

Historically, polyimide was first used in microelectronics as an insulator and then as a packaging material for planarization in multilevel interconnects [219–221] and to form multichip modules [222]. Another early application of polyimide was as molded grating patterned x-ray masks [223]. Later, polyimides gained popularity as a MEMS material. Early applications explored the use of the polymer as a flexible substrate for sensor arrays [217] and for neuroprosthetic microelectrode arrays (in early recognition of its potential biocompatibility and biostability) [224, 225]. Polyimides for specific MEMS applications were previously briefly reviewed in [67] and later in [59].

3.1. Properties summary

Key characteristics of polyimides include high glass transition temperature, high thermal stability (up to 400 °C), low dielectric constant, high mechanical strength, low modulus, low moisture absorption, chemical stability and solvent resistance [57–59]. This combination of features led to its introduction in electronics as a replacement for ceramics [58] and as a more versatile electroplating mask for use with both alkaline or acidic baths [62]. The chemical and thermal stability of polyimides also make them an attractive sacrificial layer material [95]. Electrical and mechanical properties are reviewed in [218] and characterization of the mechanical properties in thin films was performed in [226]. Because of its chemical structure, polyimides can accept various degrees of chemical modification, allowing it to be tailored for various applications [60, 61]—e.g. modification of its electrical properties has been investigated by adding graphite particles for piezoresistive sensing applications [227]. Polyimides can also come in photosensitized formulations to produce positive or negative photoresists for lithographic patterning of high aspect ratio structures with sharp sidewalls [62]. The multiple forms of polyimide commonly used for MEMS applications are commercially available from HD MicroSystems (Parlin, NJ) and DuPont (Wilmington, DE).

For biological applications, favorable mechanical properties such as flexibility, inertness [77], and low cytotoxicity [79] have all been cited as reasons for selection of polyimide over other traditional rigid MEMS materials. Recently, the

biocompatibility of polyimide was assessed and confirmed in [63] and [64, 65].

3.2. Micromachining strategies

3.2.1. Photopatterning strategies. Photosensitive polyimides take advantage of a polyamic acid precursor that can be patterned using standard photolithographic processes as both positive or negative tones depending on the polymeric structure [60, 66]. Following spin and initial softbake, UV exposure can be used to pattern this photosensitive layer, and unexposed/exposed regions are developed away using a solvent (also depending on the formulation). The final structures are then cured to complete the imidization process and form the polyimide polymer. This curing temperature (300–500 °C) however, can be prohibitively high when considering thermal budget limitations of some MEMS materials; localized curing using MEMS microheaters [228] has been explored to successfully cure specific regions of polyimide on wafer. Though convenient, these photo-definable polyimides are limited to structures that can be photolithographically defined [72] and also suffer from bulk shrinkage during the imidization process [62, 218]; etching methods are preferred to lithographic patterning to produce high resolution structures.

As conventional exposure systems and lithography can be time-consuming and expensive in creating 3D structures out of polyimide, maskless and direct writing technologies have been developed as a faster and more convenient alternative. A maskless system was used in the grayscale lithography of positive tone polyimide [229], demonstrating the possibilities of constructing multi-level 3D structures in a single spin. Direct printing of polyimide was also exhibited using a modified needle-based micropen to extrude polyamic acid onto the substrate [230]. Viscosity modifications to allow for direct writing was made by adding solvents to the polyamic acid solution.

3.2.2. Removal strategies. Similar to SU-8 films, cured polyimides are difficult to remove by wet etching, but removal using hot bases and very strong acids has been reported [218]. A combination of sulfuric acid and hydrogen peroxide was successful in removing 1 μm thick sacrificial polyimide islands with good selectivity against silicon nitride and oxide [231]. Ozone solutions have also been explored [174]. The removal of uncured polyimides (i.e. not imidized) by wet etching has been accomplished in potassium hydroxide (KOH) solutions (5–30%) [62, 67, 232, 233].

More practical polyimide removal is achieved by conventional dry etching techniques. Commonly used plasmas are formed from O_2 gas alone [234] or in combination with CF_4 , CHF_3 , and SF_6 gases [67–73]. Al is most commonly used as a hard mask [67, 69, 71, 77, 81, 95, 235]; Cr/Au [70], PECVD silicon nitride [236], oxide [95], and silicon carbide (SiC) [95] have also been explored. It has been noted that oxide masks may be superior to Al and SiC due to stronger adhesion to polyimide and easier removal, respectively [95]; oxide has also been preferred due to its lower residual stress [96]. Plasma

etching has also been used for removal of polyimide sacrificial layers [96]. O_2 plasma treatment has successfully released rotating structures, comb drives, accelerometers, electrothermal actuators [95], and pressure sensors [237] fabricated using Al, Ti, silicon nitride, and PECVD SiC structural layers with polyimide sacrificial layers.

A brief note is required here on observed plasma-induced damages to polyimide films following plasma treatment. Fluorine-based chemistry plasmas typically used to etch silicon have been found to alter the material properties of polyimide films following the etch: namely, an increase in surface roughness (e.g. an increase from 0.86 to 23.9 nm mean surface roughness, which varies with process parameters) [73, 238], loss of transparency, and the addition of fluorine units within the chemical structure [239].

Control of sidewall profile angle is possible by varying gas concentrations, plasma power, and ambient pressure [240–243]. High aspect ratios have been reported for patterning polyimides with an electron-cyclotron resonance source and O_2 plasma [244]. For a systematic study of reactive ion etching of polyimide foils (Kapton) that cannot be photolithographically patterned or removed by wet etching, the reader is referred to [245] in which O_2/SF_6 plasmas and Al hard masks were employed. Removal of uncured films using dry etching techniques has also been reported [67]. Direct write etching of polyimide using a microplasma jet in air has also been demonstrated, removing the need for etch masks [246].

Other nonconventional dry removal techniques include focused ion beam (FIB) and excimer laser machining. FIB has been demonstrated for maskless machining of optical waveguides [69]. Excimer laser machining is more widely applied for deinsulating electrodes [247] and patterning structures [233, 248–251]; the technique is reviewed in [252]. Selective photoablation can also be used to modify surfaces for patterning of biomolecules [253].

3.2.3. Release techniques. Polyimide is frequently used as a flexible substrate or in freestanding structures released from the wafer. While it is possible to simply peel polyimide from Si wafers [77, 80, 81], this technique is not practical for all applications and thus several materials have been investigated as sacrificial layers. Release from Si substrates can be achieved by undercutting in an $\text{HF}:\text{HNO}_3$ (1 : 1) etch [224], or from SiO_x sacrificial layers by undercutting with HF [79]. For -OH terminated SiO_2 surfaces (e.g. oxidized Si or Pyrex wafers), polyimide films can be released by immersion in hot DI water followed by buffered HF (BHF). It is hypothesized that the relatively rapid rate of film release is attributed to BHF induced breakage of hydrogen bonds between the polyimide and -OH terminated SiO_2 surfaces and not etching alone [254].

Many metal sacrificial layers have also been used including Al (wet release with a mixture of phosphoric-acetic-nitric acids and water [234, 255, 256], anodic dissolution in sodium chloride [257], and electrochemical erosion [65]), thick electroplated Cu (ferric chloride release of 15–50 μm thick films) [70], Cr ($\text{HCl}:\text{H}_2\text{O}$ 1 : 1 etch) [62], and Ti (removal in dilute HF) [258, 259]. Polymers that decompose at high temperatures

such as polycarbonates [257] and polynorbonenes (PNB) [57] can also be used as sacrificial layers. These materials are removed at elevated temperatures of 300 °C and 370–425 °C, respectively, in microchannels or sealed cavities.

3.2.4. Bonding techniques. Polyimide layers can also be used in various dry bonding processes to join whole wafers or individual dies; these methods may be preferred over typical adhesive methods. An RF dielectric heating method can permanently join two Si wafers together by heating spun on polyimide films (5–24 μm thick) sandwiched between two Si wafers at the glass transition temperature (1–4 bar clamping pressure, RF level of 500W at 14 MHz, and 165–180 V_{rms}). Void free bonds were achieved by curing the polyimide prior to bonding to prevent out-gassing [260]. With polyimide adhesive layers, debonding is feasible by using warm solvents with agitation or UV laser irradiation (if one wafer is transparent) [261]. UV irradiation is hypothesized to break chemical bonds formed during the heat treatment of polyimide films, partially reverse the hardening, and lower the resistance of the polyimide to dissolution [262]. In one application, thermal inkjet printheads were assembled using electrostatic bonding of fully cured polyimide to Si (350 °C, 1 kg cm⁻² clamping pressure, and 100V); here, chemical mechanical polishing of the polyimide layer was required prior to bonding [263]. Bonding using polyimide spacers to join an optical MEMS actuation and wiring chip to a mirror array chip using flip-chip processes was demonstrated in [264]. Bonding to PDMS was also demonstrated using SiC and SiO₂ glue layers that allowed for strong covalent bonding between the polyimide and PDMS [265].

Hot embossing, or nanoimprinting, onto polyimide films has also been characterized to construct deep features (>100 μm) [74, 75]. This technique is similar to standard hot embossing of polymers utilizing a micropatterned Si mold that is pressed into the polymer substrate that is heated above its T_g ($T_g = 275$ °C for polyimide).

3.2.5. Surface and bulk modifications. Similar to SU-8, plasma treatment of polyimide surfaces have demonstrated the development of hydrophilic surfaces through the formation of oxygen radicals on the surface, such as carbonyl, alcohol, and carboxyl groups [76]. However, if a hydrophilic surface is undesired following plasma treatment, deposition of C₄F₈ can help restore hydrophobicity [76]. Ion bombardment during plasma treatment (e.g. using Ar⁺ ions) has also demonstrated the removal of intrinsic stresses by breaking and reforming polymer bonds [266]; this treatment was effective in removing stress from released polyimide cantilevers that would deform out-of-plane and restore them to their original structures.

Ion track technology has been reported for bulk film modification in which nanometer wide channels are created to span the top and bottom of the film following heavy ion irradiation at high kinetic energies [267]; these nanometer channels were used to form microvias between the top and bottom surfaces following metallization in the development of a thermoelectric sensor. Another group characterized an electrospinning

technique to form a polyimide/carbon nanotube nanocomposite that produced films with better thermal stability and mechanical strength than unmodified polyimide [268].

3.2.6. Fabrication challenges. The poor adhesion of polyimide onto certain materials, as well as vice-versa, has been noted as a processing challenge. Excellent adhesion to Cr without adhesion promotion has been reported; but for other substrates such as Si, Si-derivatives, Al, and Cu, it is possible to apply silane-based adhesion promotion agents [269]. Adhesion of thin film metals to polyimide has also been shown to be problematic (e.g. Al [95]). One technique to improve metal adhesion is through the use of adhesive layers such as SiO_x for Al [95] or Ti for Au [64] and Pt [270]. Others have noted that O₂ plasma RIE roughening of polyimide surfaces can promote metal-to-polyimide [271] and polyimide-to-polyimide adhesion [79].

Also, due to the imidization process, significant dimensional changes can occur in patterned polyimide structures. Shrinkage of features up to 20–50% during curing process have been reported [79, 95, 96] and must be taken in to account during device design. Uncured films may be used to avoid shrinkage in some applications, but many devices leverage this shrinkage phenomenon to form unique structures such as hinges (figure 3(a)) [272, 273].

3.3. Notable applications

Many of the early applications of micromachined polyimide were biomedical in nature, with a particular focus on electronic neuroprosthetic devices built on the flexible substrate for improved *in vivo* performance. Flexible polyimide substrates were used to create microelectrode arrays (MEAs) for cochlear prostheses [224, 225]. Polyimide films were also used as insulation in MEAs for electrophysiological recordings for both *in vitro* [274] and *in vivo* [275] applications. Since these early examples, many have constructed MEAs on a flexible polyimide substrate with both planar and 3D electrodes (figure 3(b)) [63, 65, 71, 77–86]. In more recent work, microfluidic channels [90] and nanoporous filters [276] have also been integrated with polyimide-based neural probes for drug delivery. Various free-film sensors have also been developed including thermal [87], tactile [88], and humidity [92] sensors that involve polyimide at the core of the sensing mechanism (e.g. polyimide as a water absorber for humidity sensor [89]) and/or as the substrate. Currently there is a great degree of effort in the development of ‘smart skins’ [254, 277–280], to add sensing functionality to a flexible ‘skin-like’ substrate made from polyimide.

One interesting subset of free-film polyimide devices is the ‘lab-on-a-tube’ technology, where sensors are integrated onto a polyimide microcatheter or microtube (figure 3(c)). These can be constructed either by fabricating planar devices and precision rolling them into a tube [91] or through surface micromachining on the curved surface of a polyimide microcatheter using 3D photolithography involving the deposition, patterning, etching, and deposition on the 3D surface [92]. In

the latter devices, nanoimprinting has also been demonstrated to form additional microdome features on the curved polyimide surfaces for improved surface area for electrochemical sensing electrodes [92].

In addition to free film devices, there are a multitude of examples in which simple mechanical structures have been micromachined from polyimide. Simple apertures etched into polyimide membranes have been used in the fabrication of suspended bilayer lipid membranes [232]. Precisely defined polyimide wells have also been constructed as sub nanoliter volume microchambers for electrochemical measurements [281, 282] and neuronal cell cavities for patch clamp experiments [283]. Diaphragms [284] and microchannels [251] for LOC applications have also been constructed. The thermal shrinkage as a consequence of the imidization process has been exploited to create hinge structures that allow out-of-plane assembly of structures. This phenomenon has been leveraged for devices capable of self-assembly [93, 94] as well as flexible hinges [285, 286] and joints for segments in a neural probe [287].

4. Parylene C

Parylene, a commercial name for poly p-xylylene, was initially described as a ‘snake-skin’ like polymer and was first synthesized by Michael Mojzesz Szwarc in 1947 [288]. It was not until the development of a stable dimer precursor and optimization of a chemical vapor deposition (CVD) process by William Gorham at Union Carbide [289] that a commercially viable form of the material was introduced. This Gorham process begins with a granular dimer precursor, di-p-xylylene, that is vaporized and then pyrolyzed at a temperature above 550 °C to cleave the dimer into its reactive radical monomer. Within the deposition chamber, the reactive monomer adsorbs to all exposed surfaces and begins to spontaneously polymerize to form conformal Parylene films. This process not only enables the control of deposition parameters (e.g. vaporizer, pyrolysis temperatures and chamber pressure), but is also conducted at room temperature, allowing compatibility with thermally sensitive materials. For a more thorough review of the deposition and polymerization process, as well as a proposed chemical model, the reader is referred to [290].

Various chemical variants of Parylenes with different functional groups are available and used within the MEMS community; there are more than 10 commercially available variants of Parylenes to date. The most common within literature are Parylene N, Parylene C, Parylene D, and Parylene HT (also named AF-4). Parylene C has been the most popular for biological applications because it was the first variant to attain ISO 10993, USP class VI rating (the highest biocompatibility rating for plastics), and has excellent water and gas barrier properties. It is important to note that Parylene N and Parylene HT have also since received the ISO-10993, USP Class VI rating. Parylene HT is also becoming more popular, largely because of its improved properties: lower dielectric constant, higher ultraviolet stability, better crevice penetration, higher thermal stability, and lower moisture absorption. Currently, the commercial market for Parylenes is led by two

companies, Specialty Coating Systems (SCS; ‘Parylene’ trade name) and Kisco Conformal Coating LLC (‘diX’ trade name). Though many chemical Parylene variants have been produced for different applications, the polymer predominantly used for bioMEMS is Parylene C (hereon referred to as Parylene) because of its properties discussed in the next session, and thus is the focus of this section of the review.

4.1. Properties summary

Much like SU-8 and polyimide, Parylenes have ideal properties for barrier applications due to their chemical inertness and uniform and conformal deposition [97, 98]. Parylene gained popularity as a MEMS material due to the advantages of its simple deposition process and compatibility with standard micromachining and photolithographic processes. The coating process is compatible with a variety of MEMS materials and structures largely due to its gas phase, pinhole-free polymerization at room temperature. The deposited film also has low to no intrinsic stress, though stresses can increase following processing methods that heat the film (e.g. plasma treatment) [99]. Parylene is also ideal for applications requiring optical transparency, as it demonstrates little optical scattering and high transmittance in the visible spectrum, much like SU-8 [100–104]. However, changes in deposition conditions can significantly alter Parylene’s material properties; control of deposition parameters has been exploited to attain Parylene with different mechanical and chemical properties [290–292]. In general, faster deposition rates were found to increase the surface roughness of Parylene [292].

Specifically for bioMEMS, Parylene has been widely adopted for its proven biocompatibility and chemical inertness which are imparted by its chemical structure. As the deposition process does not require any additives (unlike epoxies) and has no harmful by-products, Parylene has been the standard for the coating of implantable devices as well as a structural MEMS material for biomedical devices. Numerous published studies have tested the biocompatibility of Parylene both *in vitro* [120] and *in vivo* [98], and its biostability, low cytotoxicity, and resistance against hydrolytic degradation have been strong arguments for its use as a biomedical material [105–107].

4.2. Micromachining strategies

4.2.1. Deposition strategies. As mentioned previously, as the CVD of Parylene is a tunable process, variants of the standard coating method have been investigated. One common technique to form Parylene structures is the deposition onto molds—3D Parylene devices have been constructed by depositing the film onto structural molds (e.g. photoresist, silicon, PDMS) to form hemispherical, bump electrodes [293], pockets for silicon chips [294], and 3D micro electrode arrays [108–110]. One effort utilized a two-photon polymerization process to create nano/micro structures out of photoresist with high resolution (<100 nm) and coated the structures with Parylene to form precisely constructed 3D polymer structures [295].

Beyond molds, Parylene deposition onto different surfaces has also been used to fabricate films with unique properties. The Parylene on liquid deposition (PoLD) technique [111], also known as the solid on liquid deposition (SOLID) process [296], involves the deposition of Parylene on low vapor pressure liquids (e.g. glycerin, silicone) to form unique structures and films. This technique has been utilized to fabricate complex optical devices, including microliquid lenses [102], liquid prisms [103], and a micro droplet array for displays [101]. Alternatively, the liquid can serve as a sacrificial layer to fabricate microfluidic devices without the need for molds, polymer sacrificial structures, or channel bonding [297].

In addition, methods that interfere with the deposition process have also been leveraged to synthesize novel structures, including: a porous Parylene film for use as an ultrafilter that uses evaporating glycerin vapors during the deposition process to hinder polymer growth [298] and Parylene nanofibers using oblique angle polymerization (OAP), a membrane template technique that physically hinders the diffusion of the monomer units [299]. In one example, von Metzen *et al* used an aperture to impede the diffusion of monomer units, as a technique for controlled, tapered deposition of Parylene [300]. Furthermore, techniques that inhibit the adsorption of Parylene on surfaces have enabled the selective deposition of Parylene. In most cases, heat is used to prohibit the deposition of Parylene [301, 302], as a localized temperature increase ($>140\text{ }^{\circ}\text{C}$ [302]) can reduce the deposition rate in that region [303, 304]. Another technique utilized deposited transition metals (e.g. Fe, Au, Ag, Pt) that deactivate the Parylene radical monomers to delay the initiation and propagation steps of Parylene polymerization [305].

It is important to address the issue of adhesion of Parylene on different materials. Though the deposition of Parylene results in strong adhesion for many substrates, it is not universal. Adhesion can be improved through the use of A-174, a silane-based adhesion promoter, that has been found to greatly increase the adhesion of Parylene for silicon devices [141] as well as platinum surfaces [306]. Adhesion is further addressed below in the discussion on surface modification and processing challenges.

4.2.2. Removal strategies. Much like the polymers mentioned previously, etching techniques for Parylene are limited to physical and dry processes largely due to its high chemical inertness. There have been reports of the wet etching of Parylene using chloronaphthelene or benzoyl benzoate [307], but only at extreme temperatures ($>150\text{ }^{\circ}\text{C}$). Dry etching techniques have been found to be the most effective and practical to etch Parylene; for a more detailed review of plasma etching of Parylene, the authors refer the reader to [115]. Parylene etching can be accomplished using O_2 chemistry-based plasma etching [112–115], reactive ion beam etching (RIBE) [308], and reactive ion etching (RIE/deep RIE or DRIE) [115, 309, 310]. These techniques produce an isotropic etch profile, as RIE and DRIE methods can create aspect ratios of 2 : 1, while plasma etching is limited to a 1:1 ratio. A switched chemistry etch that involves cycling through (1) deposition of C_4F_8 as a

sidewall passivation layer, (2) etching in SF_6 plasma, and (3) etching in O_2 plasma similar to the standard Bosch process was found to improve the anisotropy to produce fairly vertical sidewalls [115]. Many materials have been explored as etch masks for Parylene including photoresists, Al, oxides, spun on glass, nitride, and α -silicon [115, 309–311], but photoresist and sputtered Al remain the most popular, due to ease of patterning and hard mask qualities, respectively. However, the etch selectivity between photoresist and Parylene is very low (1 : 1) and may not be optimal when etching thick Parylene layers ($>10\text{ }\mu\text{m}$) [115].

Other methods for Parylene removal include laser ablation [312–314], one of the first techniques for Parylene etching to expose electrode sites, and manual removal by peeling. For the latter, pre coating of release agents, such as Micro-90 lab cleaning solution (International Products Corporation, Burlington, NJ), on the substrate [122] as well as immersion in water [130, 131, 134] can aid in the removal of the film without damage.

4.2.3. Release techniques. Typically, Parylene can be released fairly easily using manual peeling because of poor adhesion to the native oxide layer of Si surfaces. As mentioned previously, release agents such as Micro-90 (applied before deposition) [122] or immersion in water during peeling [315, 316] can aid in the process. However, if A-174 has been applied to the substrate surface, manual release of the devices is difficult and a sacrificial release layer is necessary. Typically photoresist [135, 317, 318] or thin film metals such as Al [133, 319] or Ti [320] release layers have been utilized that can be removed via solvents or through chemical etching.

4.2.4. Bonding techniques. Application of temperature and pressure facilitates Parylene to polymer bonding for a variety of applications, such as forming microchannel structures. By exposing Parylene-polymer constructs to high temperatures (greater than the glass transition point of Parylene, $60\text{--}90\text{ }^{\circ}\text{C}$ [122]) while applying a bonding pressure, mechanical fusing of Parylene into the second polymer can be achieved for bond formation. Plasma activation of the Parylene C layer to create radical species can further aid in this process. This mechanism can be used to create Parylene to oxide bonds at $280\text{ }^{\circ}\text{C}$ with O_2 plasma treatment [125], as well as Parylene to photoresist (SU-8, AZ 4620) bonds, for temperatures greater than $90\text{ }^{\circ}\text{C}$ with O_2 plasma treatment [124]. Bonding strength was found to increase with increased bonding temperature [124]. Parylene-Parylene bonding has also been demonstrated at both die [123] and wafer [321–323] levels, to construct devices or to achieve an intermediate glue layer for wafer-level bonding.

Hot-embossing of Parylene has also been demonstrated, where a Ni mold was pressed into Parylene films at $150\text{ }^{\circ}\text{C}$ to form an imprint with $<2.32\%$ dimensional deviation [116]. Thermal forming of Parylene free films is also feasible by annealing multi-layer Parylene devices with varying thickness or differing Parylene variants (Parylene C, N structures) to create residual stress differences to form self-curling films [132, 136, 320]. Metal molds have also been used to thermally

shape Parylene planar films into curved [117, 118] and 3D structures [119].

4.2.5. Surface and bulk modification. Plasma treatment of Parylene surfaces has been explored to improve the adhesion of various materials to Parylene. Oxygen plasma and ion beam treatment of Parylene prior to gold deposition was found to increase adhesion properties largely due to the added carbonyl functional groups following the process, as well as mechanical interlocking due to increased roughness [324]. Ar, O₂, and methane *in situ* plasma treatment (i.e. plasma treatment within the Parylene deposition chamber) of poly tetrafluoroethylene (PTFE), poly propylene (PP), poly methylmethacrylate (PMMA), and glass substrates during Parylene deposition also contributed to a qualitative increase in adhesion, however the mechanisms for improved adhesion were different for each chemistry [325]. O₂ plasma treatment of PDMS has also been observed to increase Parylene adhesion up to a four-fold improvement [326].

O₂ plasma treatment can also be utilized to create hydrophilic Parylene surfaces by introducing oxygen-related polar functional groups (e.g. carboxyl, hydroxyl) onto the surface, but the hydrophobic nature of Parylene (native contact angle 80–90°) was found to revert to 40–50% of its initial state following a week [327]. Consecutive O₂-SF₆ (COS) plasma treatment has been found to achieve contact angles of 169.4° to create super-hydrophobic surfaces, stemming from O₂ plasma induced surface roughening and fluorine-based chemical modification of the surface with SF₆ [328].

For bioMEMS, plasma treatment of Parylene C surfaces can improve cell adhesion, typically poor for untreated Parylene surfaces [120, 121]. Another method to improve cellular adhesion is to adhere proteins onto as-deposited Parylene films (e.g. horse serum, bovine serum albumin, immunoglobulin G, fibronectin, Matrigel) by soaking the films within the solution [120, 329]. Other methods for surface modification of Parylene C for biomedical applications involve UV-induced photooxidation (1 or 2 h treatment) to create a hydrophilic surfaces by producing carboxyl and aldehyde groups [329]. The addition of other functional groups to the polymer surface using Friedel-Crafts acylation to add thiol and poly N-isopropylacrylamide (pNIPAM) groups for improved gold film and tissue adhesion, respectively has also been demonstrated [330].

4.2.6. Fabrication challenges. The relatively narrow range of processing temperatures compatible with Parylene is a large fabrication challenge as any process that nears the T_g of Parylene can induce bulk material changes that can greatly affect processing [122]. For example, standard soft bake temperatures for photoresists spun on silicon wafers are ~120 °C; for Parylene, this temperature must be reduced. Similarly during O₂ plasma dry etching, cooling or rest steps must be included to prevent Parylene from being exposed to temperatures above its T_g for long periods of time due to heating from the plasma exposure. These thermal considerations extend to optimal operating conditions of Parylene C devices; mismatch of coefficient of thermal expansion (CTE) between Parylene

and the coated substrate has been found to result in mechanical failure for devices under relatively high temperature soaking conditions [331].

It is also well established that the adhesion between Parylene-Parylene layers and Parylene-metal (e.g. thin film gold, titanium, platinum) layers can be compromised during long term soaking conditions, with device life lasting from days [137–140] to more than a year [141]. Soaking induced delamination is strongly dependent on the presence of voids or contaminants at the bond interface [332]. This motivates additional cleaning processes prior to Parylene deposition (e.g. dilute HF bath [333]) to prevent void formation. In light of this, efforts to improve the adhesion between Parylene-Parylene and Parylene-metal layers have largely focused on annealing via *in situ* heating [334] as well as a post-treatment [117, 134, 335] and plasma treatment (as mentioned previously).

4.3. Notable applications

Parylene devices, both structural and free film, are largely associated with bioMEMS due to the outstanding biocompatibility and optimal material properties of the polymer for biomedical applications. As hybrid devices, traditional LOC structures such as Parylene microchannels [122–125] or cell chips [316] have been constructed using standard Parylene deposition on mold techniques. Parylene films have also been used as the critical elements of these devices, including membranes for pressure sensors [126], sensing elements of pH sensors [127], semipermeable diffusion membranes for cell chips [336], and a bellows-type diaphragm element for a drug delivery device [337–339]. Parylene hybrid devices have also been designed as novel cortical probes to record electrical signals from neurons (figure 4(a)). These devices combine the biocompatible and flexible nature of Parylene with rigid silicon [109, 340, 341], metal [319], or SU-8 [342] regions to add stiffness for easier insertion into cortical tissue.

Parylene free film devices are predominantly constructed as a flexible Parylene substrate with Parylene structural elements. One advantage of Parylene free film devices is that the fabrication process is compatible with the integration of transducer, electrical components (e.g. coils [137, 343], discrete electronics [135], and chips [135, 294]), and flexible electrical connections (e.g. cable) into a single, encapsulated structure, constructing all elements of the device on wafer. This type of technology has been prominent in the field of neural prosthetics where Parylene-based neural electrodes in both penetrating (figure 4(b)) [130, 131] and non-penetrating orientations [104, 344, 345], in addition to cuff [132, 133] and spinal cord stimulators [335] have been developed. Parylene-based retinal (figure 4(c)) [108, 134, 135] and cochlear [136] implants have also been constructed, where thermal shaping of Parylene allowed for the matching of biological curvatures while leveraging Parylene processing to create high density electrode arrays. One novel Parylene-based sensor technology involves an electrolyte-filled, Parylene microchamber-based force sensor that utilizes changes in electrochemical impedance to measure deflections of Parylene membranes [128, 129].

A similar sensing paradigm was utilized in the development of a Parylene-based pressure sensor that employed a unique microbubble-based sensing mechanism to measure hydrostatic pressure [346, 347].

5. Conclusion and perspectives

Within this review, a high-level overview of widely used and recently developed micromachining strategies and examples of some notable microdevices for three of the polymers typically used for MEMS (i.e. SU-8, polyimide, and Parylene) was presented. It is through these micromachining techniques in the development of novel polymer-based devices that the field of polymer-MEMS has proliferated rapidly in recent years. However, though these polymers provide many advantages as a structural and substrate material for micro-machined devices, many processing challenges remain that require further investigation. Despite the limitations that have been revealed to date, the outlook for polymers in MEMS is promising as they offer a wide range of tunable and desirable properties. Continued process development is expected to resolve many existing issues and it is also anticipated that new microfabrication-compatible polymers will also be introduced that will further expand polymer applications in MEMS.

Acknowledgments

This work was funded by the NSF under award number EFRI-1332394. The authors would also like to acknowledge the members of the Biomedical Microsystems Laboratory at the University of Southern California for their insightful thoughts and discussion in the preparation of this review.

References

- [1] Xia Y and Whitesides G M 1998 Soft lithography *Annu. Rev. Mater. Sci.* **28** 153–84
- [2] Mata A *et al* 2005 Characterization of polydimethylsiloxane (PDMS) properties for biomedical micro/nanosystems *Biomed. Microdevices* **7** 281–93
- [3] Wang X *et al* 2003 Liquid crystal polymer (LCP) for MEMS: processes and applications *J. Micromech. Microeng.* **13** 628
- [4] Nunes P S *et al* 2010 Cyclic olefin polymers: emerging materials for lab-on-a-chip applications *Microfluid. Nanofluidics* **9** 145–61
- [5] Becker H and Heim U 2000 Hot embossing as a method for the fabrication of polymer high aspect ratio structures *Sensors Actuators A* **83** 130–5
- [6] Grayson A C R *et al* 2004 A BioMEMS review: MEMS technology for physiologically integrated devices *Proc. IEEE* **92** 6–21
- [7] Ziaie B *et al* 2004 Hard and soft micromachining for BioMEMS: review of techniques and examples of applications in microfluidics and drug delivery *Adv. Drug Deliv. Rev.* **56** 145–72
- [8] Liu C 2007 Recent developments in polymer MEMS *Adv. Mater.* **19** 3783–90
- [9] Becker H and Gärtner C 2008 Polymer microfabrication technologies for microfluidic systems *Anal. Bioanal. Chem.* **390** 89–111
- [10] Kim P *et al* 2008 Soft lithography for microfluidics: a review *Biochip J.* **2** 1–11
- [11] Shaw J M *et al* 1997 Negative photoresists for optical lithography *IBM J. Res. Dev.* **41** 81–94
- [12] Jiguet S *et al* 2004 SU8-silver photosensitive nanocomposite *Adv. Eng. Mater.* **6** 719–24
- [13] Jiguet S *et al* 2005 Conductive SU8 photoresist for microfabrication *Adv. Funct. Mater.* **15** 1511–6
- [14] Damean N *et al* 2005 Composite ferromagnetic photoresist for the fabrication of microelectromechanical systems *J. Micromech. Microeng.* **15** 29–34
- [15] Foulds I G and Parameswaran M 2006 A planar self-sacrificial multilayer SU-8-based MEMS process utilizing a UV-blocking layer for the creation of freely moving parts *J. Micromech. Microeng.* **16** 2109–15
- [16] Ruano-Lopez J M *et al* 2006 A new SU-8 process to integrate buried waveguides and sealed microchannels for a Lab-on-a-Chip *Sensors Actuators B* **114** 542–51
- [17] Jiguet S *et al* 2006 Effect of filler behavior on nanocomposite SU8 photoresist for moving micro-parts *Microelectron. Eng.* **83** 1273–6
- [18] Jiguet S *et al* 2006 SU-8 nanocomposite coatings with improved tribological performance for MEMS *Surf. Coat. Technol.* **201** 2289–95
- [19] Jiguet S *et al* 2006 SU-8 nanocomposite photoresist with low stress properties for microfabrication applications *Microelectron. Eng.* **83** 1966–70
- [20] Jiang L *et al* 2008 An SU-8 based fluidic immunospectroscopic lab-on-a-chip for rapid quantitative detection of biomolecules *IEEE 21st Int. Conf. on Micro Electro Mechanical Systems* pp 204–7
- [21] Yang B *et al* 2009 Fabrication and characterization of small optical ridge waveguides based on SU-8 polymer *J. Lightwave Technol.* **27** 4091–6
- [22] Despont M *et al* 1997 *High-Aspect-Ratio, Ultrathick, Negative-Tone Near-Uv Photoresist for MEMS Applications* (Nagoya, Japan) pp 518–22
- [23] Guerin L J *et al* 1997 Simple and low cost fabrication of embedded micro-channels by using a new thick-film photoplastic *Transducers 1997* vol **2** (Chicago, IL, USA: IEEE) pp 1419–22
- [24] Bohl B *et al* 2005 Multi-layer SU-8 lift-off technology for microfluidic devices *J. Micromech. Microeng.* **15** 1125–30
- [25] Jackman R J *et al* 2001 Microfluidic systems with on-line UV detection fabricated in photodefinable epoxy *J. Micromech. Microeng.* **11** 263–9
- [26] Mata A *et al* 2006 Fabrication of multi-layer SU-8 microstructures *J. Micromech. Microeng.* **16** 276–84
- [27] Kuo J T and Meng E 2012 Improved process for high yield 3D inclined SU-8 structures on soda lime substrate towards applications in optogenetic studies *2012 IEEE 25th Int. Conf. on Micro Electro Mechanical Systems* pp 263–6
- [28] Yoon Y-K *et al* 2006 Multidirectional UV lithography for complex 3-D MEMS structures *J. Microelectromech. Syst.* **15** 1121–30
- [29] Zhao J *et al* 2012 Surface treatment of polymers for the fabrication of all-polymer MEMS devices *Sensors Actuators A* **187** 43–9
- [30] Aracil C *et al* 2010 BETTS: bonding, exposing and transferring technique in SU-8 for microsystems fabrication *J. Micromech. Microeng.* **20** 035008
- [31] Hong G *et al* 2004 SU8 resist plasma etching and its optimisation *Microsyst. Technol.* **10** 357–9
- [32] Lorenz H *et al* 1998 Fabrication of photoplastic high-aspect ratio microparts and micromolds using SU-8 UV resist *Microsyst. Technol.* **4** 143–6
- [33] Zhang J *et al* 2001 Polymerization optimization of SU-8 photoresist and its applications in microfluidic systems and MEMS *J. Micromech. Microeng.* **11** 20–26

- [34] Duffy D C *et al* 1998 Rapid prototyping of microfluidic systems in poly (dimethylsiloxane) *Anal. Chem.* **70** 4974–84
- [35] Abgrall P and Gue A M 2007 Lab-on-chip technologies: making a microfluidic network and coupling it into a complete microsystem—a review *J. Micromech. Microeng.* **17** R15–R49
- [36] Arscott S 2014 SU-8 as a material for lab-on-a-chip-based mass spectrometry *Lab Chip* **14** 3668–89
- [37] Chaudhuri B P *et al* 2013 A novel method for monolithic fabrication of polymer microneedles on a platform for transdermal drug delivery 2013 35th Annual Int. Conf. of the IEEE Engineering in Medicine and Biology Society pp 156–9
- [38] Wang P-C *et al* 2013 Fabrication and characterization of polymer hollow microneedle array using UV lithography into micromolds *J. Microelectromech. Syst.* **22** 1041–53
- [39] Kwon K and Li W 2013 Integrated multi-LED array with 3D polymer waveguide for optogenetics 2013 IEEE 26th Int. Conf. on Micro Electro Mechanical Systems pp 1017–20
- [40] Fiedler E *et al* 2014 Suitability of SU-8, Epoclad and Epocore for flexible waveguides on implantable neural probes 2014 36th Annual Int. Conf. of the IEEE Engineering in Medicine and Biology Society pp 438–41
- [41] Kwon K Y *et al* 2013 Droplet backside exposure for making slanted SU-8 microneedles 2013 35th Annual Int. Conf. of the IEEE Engineering in Medicine and Biology Society pp 767–70
- [42] Chung S and Park S 2013 Effects of temperature on mechanical properties of SU-8 photoresist material *J. Mech. Sci. Technol.* **27** 2701–7
- [43] Lukes S J and Dickensheets D L 2013 SU-8 2002 surface micromachined deformable membrane mirrors *J. Microelectromech. Syst.* **22** 94–106
- [44] Eyre B *et al* 1998 Taguchi optimization for the processing of Epon SU-8 resist 11th Ann. Int. Workshop on Micro Electro Mechanical Systems (Heidelberg, Germany) pp 218–22
- [45] Chang H K and Kim Y K 2000 UV-LIGA process for high aspect ratio structure using stress barrier and C-shaped etch hole *Sensors Actuators A* **84** 342–50
- [46] Ling Z-G *et al* 2000 Improved patterning quality of SU-8 microstructures by optimizing the exposure parameters *Proc. SPIE 3999, Advances in Resist Technology and Processing (Santa Clara, CA, USA)* pp 1019–27
- [47] Ruhmann R *et al* 2001 Reduction of internal stress in a SU-8-like negative tone photoresist for MEMS applications by chemical modification 26th Annual Int. Symp. on Microlithography (Santa Clara, CA, USA) pp 502–10
- [48] Johnson A W *et al* 2001 Improving the process capability of SU-8. II *J. Photopolym. Sci. Technol.* **14** 689–94
- [49] Johnson D W *et al* 2002 Improving the process capability of SU-8, part III *J. Photopolym. Sci. Technol.* **15** 749–56
- [50] Shaw M *et al* 2003 Improving the process capability of SU-8 *Microsyst. Technol.* **10** 1–6
- [51] Feng R and Farris R J 2003 Influence of processing conditions on the thermal and mechanical properties of SU8 negative photoresist coatings *J. Micromech. Microeng.* **13** 80–8
- [52] Johari S *et al* 2014 The effect of softbaking temperature on SU-8 photoresist performance 2014 IEEE Int. Conf. on Semiconductor Electronics pp 467–70
- [53] Oerke A *et al* 2014 Micro molding for double-sided micro structuring of SU-8 resist *Microsyst. Technol.* **20** 593–8
- [54] Daniel J H 2001 Micro-electro-mechanical system fabrication technology applied to large area x-ray image sensor arrays *J. Vac. Sci. Technol. A* **19** 1219–23
- [55] Abgrall P *et al* 2006 A novel fabrication method of flexible and monolithic 3D microfluidic structures using lamination of SU-8 films *J. Micromech. Microeng.* **16** 113–21
- [56] Lau K H *et al* 2013 Releasing high aspect ratio SU-8 microstructures using AZ photoresist as a sacrificial layer on metallized Si substrates *Microsyst. Technol.* **19** 1863–71
- [57] Bhusari D *et al* 2001 Fabrication of air-channel structures for microfluidic, microelectromechanical, and microelectronic applications *J. Microelectromech. Syst.* **10** 400–8
- [58] Gad-el-Hak M 2006 *MEMS: design and fabrication* 2nd edn (Boca Raton, FL: CRC)
- [59] Frazier A B 1995 Recent applications of polyimide to micromachining technology *IEEE Trans. Ind. Electron.* **42** 442–8
- [60] Wilson W C and Atkinson G M 2007 Review of polyimides used in the manufacturing of micro systems *Technical Memorandum NASA/TM-2007-214870* 2007
- [61] Othman M B H *et al* 2008 Fabrication of nanoporous polyimide of low dielectric constant 2008 33rd IEEE/CPMT Int. Electronic Manufacturing Technology Symp. pp 1–4
- [62] Frazier A B and Allen M G 1993 Metallic microstructures fabricated using photosensitive polyimide electroplating molds *J. Microelectromech. Syst.* **2** 87–94
- [63] Lago N *et al* 2007 Assessment of biocompatibility of chronically implanted polyimide and platinum intrafascicular electrodes *IEEE Trans. Biomed. Eng.* **54** 281–90
- [64] Bae S H *et al* 2012 *In vitro* biocompatibility of various polymer-based microelectrode arrays for retinal prosthesis *Invest. Ophthalmol. Vis. Sci.* **53** 2653–7
- [65] Jiang X *et al* 2013 *In vitro* and *in vivo* evaluation of a photosensitive polyimide thin-film microelectrode array suitable for epiretinal stimulation *J. NeuroEng. Rehabil.* **10** 48
- [66] Fukukawa K-i and Ueda M 2008 Recent progress of photosensitive polyimides *Polym. J.* **40** 281
- [67] Frazier A B *et al* 1994 Development of micromachined devices using polyimide-based processes *Sensors Actuators A* **45** 47–55
- [68] Schubert P J and Nevin J H 1985 A polyimide-based capacitive humidity sensor *IEEE Trans. Electron Devices* **32** 1220–3
- [69] Selvaraj R *et al* 1998 Integrated optical wave-guides in polyimide for wafer scale integration *J. Lightwave Technol.* **6** 1034–44
- [70] Kim Y W and Allen M G 1992 Single-layer and multilayer surface-micromachined platforms using electroplated sacrificial layers *Sensors Actuators A* **35** 61–8
- [71] Stieglitz T *et al* 1997 A flexible, light-weight multichannel sieve electrode with integrated cables for interfacing regenerating peripheral nerves *Sensors Actuators A* **60** 240–3
- [72] Bliznetsov V *et al* 2011 High-throughput anisotropic plasma etching of polyimide for MEMS *J. Micromech. Microeng.* **21** 067003
- [73] Chen Y *et al* 2014 Fabrication of polyimide sacrificial layers with inclined sidewalls based on reactive ion etching *AIP Adv.* **4** 031328
- [74] Ikoma R *et al* 2012 Transfer of relatively large microstructures on polyimide films using thermal nanoimprinting *J. Photopolym. Sci. Technol.* **25** 255–60
- [75] Fukushi Y *et al* 2013 Fabrication and characterization of glucose fuel cells with a microchannel fabricated on flexible polyimide film *J. Photopolym. Sci. Technol.* **26** 303–8
- [76] Scheen G *et al* 2011 Simultaneous fabrication of superhydrophobic and superhydrophilic polyimide surfaces with low hysteresis *Langmuir* **27** 6490–5

- [77] Stieglitz T 2001 Flexible biomedical microdevices with double-sided electrode arrangements for neural applications *Sensors Actuators A* **90** 203–11
- [78] Stieglitz T and Gross M 2002 Flexible BIOMEMS with electrode arrangements on front and back side as key component in neural prostheses and biohybrid systems *Sensors Actuators B* **83** 8–14
- [79] Rousche P J *et al* 2001 Flexible polyimide-based intracortical electrode arrays with bioactive capability *IEEE Trans. Biomed. Eng.* **48** 361–71
- [80] Gross M *et al* 2002 Micromachining of flexible neural implants with low-ohmic wire traces using electroplating *Sensors Actuators A* **96** 105–10
- [81] Stieglitz T *et al* 2002 A biohybrid system to interface peripheral nerves after traumatic lesions: design of a high channel sieve electrode *Biosens Bioelectron.* **17** 685–96
- [82] Hanein Y *et al* 2003 High-aspect ratio submicrometer needles for intracellular applications *J. Micromech. Microeng.* **13** S91–5
- [83] Lee K *et al* 2004 Polyimide based neural implants with stiffness improvement *Sensors Actuators B* **102** 67–72
- [84] Schanze T *et al* 2007 An optically powered single-channel stimulation implant as test-system for chronic biocompatibility and biostability of miniaturized retinal vision prostheses *IEEE Trans. Biomed. Eng.* **54** 983–92
- [85] Lee S H *et al* 2009 Fabrication and characteristics of the implantable and flexible nerve cuff electrode for neural interfaces *4th Int. IEEE/EMBS Conf. on Neural Engineering* pp 80–3
- [86] Xue N *et al* 2015 Polymeric C-shaped cuff electrode for recording of peripheral nerve signal *Sensors Actuators B* **210** 640–8
- [87] Niimi Y *et al* 2014 Polymer micromachining based on Cu On polyimide substrate and its application to flexible MEMS sensor *2014 IEEE 27th Int. Conf. on Micro Electro Mechanical Systems* pp 528–31
- [88] Kilaru R *et al* 2013 NiCr MEMS tactile sensors embedded in polyimide toward smart skin *J. Microelectromech. Syst.* **22** 349–55
- [89] Choi K S *et al* 2014 A highly sensitive humidity sensor with a novel hole array structure using a polyimide sensing layer *RSC Adv.* **4** 32075–80
- [90] Metz S *et al* 2004 Flexible polyimide probes with microelectrodes and embedded microfluidic channels for simultaneous drug delivery and multi-channel monitoring of bioelectric activity *Biosens. Bioelectron.* **19** 1309–18
- [91] Li C *et al* 2007 Flexible biosensors on spirally rolled micro tube for cardiovascular *in vivo* monitoring *Biosens. Bioelectron.* **22** 1988–93
- [92] Yang Z *et al* 2014 A novel MEMS compatible lab-on-a-tube technology *Lab Chip* **14** 4604–8
- [93] Suzuki K *et al* 2007 Self-assembly of 3D micro mechanisms using thermal shrinkage of polyimide *Microsyst. Technol.* **13** 1047–53
- [94] Chen J and Liu C 2003 Development and characterization of surface micromachined, out-of-plane hot-wire anemometer *J. Microelectromech. Syst.* **12** 979–88
- [95] Bagolini A *et al* 2002 Polyimide sacrificial layer and novel materials for post-processing surface micromachining *J. Micromech. Microeng.* **12** 385–9
- [96] Ma S *et al* 2009 Study of polyimide as sacrificial layer with O₂ plasma releasing for its application in MEMS capacitive FPA fabrication *Int. Conf. on Electronic Packaging Technology & High Density Packaging* pp 526–9
- [97] Loeb G E *et al* 1977 Parylene as a chronically stable, reproducible microelectrode insulator *IEEE Transactions on Biomed. Eng.* **BME-24** 121–8
- [98] Schmidt E M *et al* 1988 Long-term implants of Parylene-C coated microelectrodes *Med. Biol. Eng. Comput.* **26** 96–101
- [99] Zöpfl T *et al* 2009 Characterisation of the intrinsic stress in micromachined parylene membranes *Proc. SPIE Europe Microtechnologies for the New Millennium* pp 73621M
- [100] Lee G-B *et al* 2003 Micro flow cytometers with buried SU-8/SOG optical waveguides *Sensors Actuators A* **103** 165–70
- [101] Binh-Khiem N *et al* 2008 Active parylene-encapsulated droplets for displays *Polym. Prepr.* **49** 931
- [102] Binh-Khiem N *et al* 2008 Polymer thin film deposited on liquid for varifocal encapsulated liquid lenses *Appl. Phys. Lett.* **93** 124101
- [103] Yoshihata Y *et al* 2009 Micro liquid prism *IEEE 22nd Int. Conf. on Micro Electro Mechanical Systems* pp 967–70
- [104] Ledochowitsch P *et al* 2011 A transparent μ ECoG array for simultaneous recording and optogenetic stimulation *2011 Annual Int. Conf. of the IEEE Engineering in Medicine and Biology Society* pp 2937–40
- [105] Kroschwitz J I 1998 *Kirk-Othmer Encyclopedia of Chemical Technology* (New York: Wiley)
- [106] Lahann J 2006 Vapor-based polymer coatings for potential biomedical applications *Polym. Int.* **55** 1361–70
- [107] Weisenberg B A and Mooradian D L 2002 Hemocompatibility of materials used in microelectromechanical systems: platelet adhesion and morphology *in vitro J. Biomed. Mater. Res.* **60** 283–291
- [108] Wang R *et al* 2010 Fabrication and characterization of a parylene-based 3D microelectrode array for use in retinal prosthesis *J. Microelectromech. Syst.* **19** 367–74
- [109] Wang R *et al* 2011 Fabrication and properties of 3D flexible parylene-based microelectrode array with silicon tips *2011 IEEE 24th Int. Conf. on Micro Electro Mechanical Systems* pp 253–6
- [110] Nishinaka Y *et al* 2013 Fabrication of polymer microneedle electrodes coated with nanoporous parylene *Japan. J. Appl. Phys.* **52** 06GL10
- [111] Binh-Khiem N *et al* 2010 Tensile film stress of parylene deposited on liquid *Langmuir* **26** 18771–5
- [112] Nowlin T E and Smith D F Jr 1980 Surface characterization of plasma-treated poly-p-xylylene films *J. Appl. Polym. Sci.* **25** 1619–32
- [113] Wang X Q *et al* 1999 A parylene micro check valve *Proc. of the IEEE Microelectromechanical Systems Conf. (Orlando, FL)* pp 177–82
- [114] Levy B P *et al* 1986 Definition of the geometric area of a microelectrode tip by plasma-etching of parylene *IEEE Trans. Biomed. Eng.* **33** 1046–9
- [115] Meng E *et al* 2008 Plasma removal of parylene *J. Micromech. Microeng.* **18** 045004
- [116] Youn S W *et al* 2007 Fabrication of a micro patterned parylene-C master by hot-embossing and its application to metallic mold replication *J. Micromech. Microeng.* **17** 1402–13
- [117] Li W *et al* 2005 Integrated flexible ocular coil for power and data transfer in retinal prostheses *27th Annual Int. Conf. of the Engineering in Medicine and Biology Society* pp 1028–31
- [118] Huang R and Tai Y-C 2010 Flexible parylene-based 3-D coiled cable *2010 5th IEEE Int. Conf. on Nano/Micro Engineered and Molecular Systems* pp 317–20
- [119] Kim B *et al* 2014 Formation of 3D Parylene C structures via thermoforming *J. Micromech. Microeng.* **24** 065003

- [120] Chang T Y *et al* 2007 Cell and protein compatibility of parylene-C surfaces *Langmuir* **23** 11718–25
- [121] Hoshino T *et al* 2012 Improvement of neuronal cell adhesiveness on parylene with oxygen plasma treatment *J. Biosci. Bioeng.* **113** 395–8
- [122] Noh H S *et al* 2004 Parylene micromolding, a rapid and low-cost fabrication method for parylene microchannel *Sensors Actuators B* **102** 78–85
- [123] Ziegler D *et al* 2006 Fabrication of flexible neural probes with built-in microfluidic channels by thermal bonding of parylene *J. Microelectromech. Syst.* **15** 1477–82
- [124] Chang J-C *et al* 2013 A low-temperature parylene-C-to-silicon bonding using photo-patternable adhesives and its applications *The 17th Int. Conf. on Solid-State Sensors, Actuators and Microsystems (TRANSDUCERS & EUROSENSORS XXVII)* pp 2217–20
- [125] Ciftlik A T and Gijs M 2011 A low-temperature parylene-to-silicon dioxide bonding technique for high-pressure microfluidics *J. Micromech. Microeng.* **21** 035011
- [126] Assadsangabi B *et al* 2014 Ferrofluid sacrificial microfabrication of capacitive pressure sensors *IEEE Sens. J.* **14** 3442–7
- [127] Aoki H *et al* 2012 Functionalized micro bead with liquid-core Parylene-shell structure *2012 IEEE 25th Int. Conf. on Micro Electro Mechanical Systems* pp 831–4
- [128] Gutierrez C A and Meng E 2011 Impedance-based force transduction within fluid-filled parylene microstructures *J. Microelectromech. Syst.* **20** 1098–108
- [129] Kim B J *et al* 2012 Parylene-based electrochemical-MEMS force sensor array for assessing neural probe insertion mechanics *2012 IEEE 25th Int. Conf. on Micro Electro Mechanical Systems* pp 124–7
- [130] Kim B J *et al* 2013 3D Parylene sheath neural probe for chronic recordings *J. Neural Eng.* **10** 045002
- [131] Kuo J T W *et al* 2013 Novel flexible parylene neural probe with 3D sheath structure for enhancing tissue integration *Lab Chip* **13** 554–61
- [132] Kang X *et al* 2015 Self-closed parylene cuff electrode for peripheral nerve recording *J. Microelectromech. Syst.* **24** 319–32
- [133] Yu H *et al* 2014 A parylene self-locking cuff electrode for peripheral nerve stimulation and recording *J. Electromech. Syst.* **23** 1025–35
- [134] Rodger D C *et al* 2008 Flexible parylene-based multielectrode array technology for high-density neural stimulation and recording *Sensors Actuators B* **132** 449–60
- [135] Li W *et al* 2011 Parylene-based integrated wireless single-channel neurostimulator *Sensors Actuators A* **166** 193–200
- [136] Johnson A C and Wise K D 2012 A self-curling monolithically-backed active high-density cochlear electrode array *2012 IEEE 25th Int. Conf. on Micro Electro Mechanical Systems* pp 914–7
- [137] Li W *et al* 2006 Flexible parylene packaged intraocular coil for retinal prostheses *Proc. of 2006 Int. Conf. on Microtechnologies in Medicine and Biology (Okinawa, Japan)* pp 105–8
- [138] Li W, Rodger D C, Menon P R and Tai Y C 2008 Corrosion behavior of parylene-metal-parylene thin films in saline *ECS Trans.* **11** 1–6
- [139] Seymour J P *et al* 2009 The insulation performance of reactive parylene films in implantable electronic devices *Biomaterials* **30** 6158–67
- [140] von Metzen R P and Stieglitz T 2013 The effects of annealing on mechanical, chemical, and physical properties and structural stability of Parylene C *Biomed. Microdevices* **15** 727–35
- [141] Hsu J M *et al* 2009 Encapsulation of an Integrated Neural Interface Device With Parylene C *IEEE Trans. Biomed. Eng.* **56** 23–9
- [142] Gelorme J D *et al* 1989 Photoresist composition and printed circuit boards and packages made therewith *US Patent* 4882245
- [143] LaBianca N C and Gelorme J D 1995 High-aspect-ratio resist for thick-film applications *Proc. SPIE 1995 Symp. on Microlithography (Santa Clara, CA, USA)* pp 846–52
- [144] Lee K Y *et al* 1995 Micromachining applications of a high resolution ultrathick photoresist *J. Vac. Sci. Technol. B* **13** 3012–6
- [145] Nemani K V *et al* 2013 *In vitro* and *in vivo* evaluation of SU-8 biocompatibility *Mater. Sci. Eng. C* **33** 4453–9
- [146] Martinez-Duarte R 2014 SU-8 Photolithography as a Toolbox for Carbon MEMS *Micromachines* **5** 766–82
- [147] Lorenz H *et al* 1997 SU-8: a low-cost negative resist for MEMS *J. Micromech. Microeng.* **7** 121–4
- [148] Abgrall P *et al* 2007 SU-8 as a structural material for labs-on-chips and microelectromechanical systems *Electrophoresis* **28** 4539–51
- [149] del Campo A and Greiner C 2007 SU-8: a photoresist for high-aspect-ratio and 3D submicron lithography *J. Micromech. Microeng.* **17** R81
- [150] Lee J B *et al* 2014 Innovative SU-8 Lithography Techniques and Their Applications *Micromachines* **6** 1–18
- [151] Bandi T *et al* 2013 Proton-radiation tolerance of silicon and SU-8 as structural materials for high-reliability MEMS *J. Microelectromech. Syst.* **22** 1395–402
- [152] Kotzar G *et al* 2002 Evaluation of MEMS materials of construction for implantable medical devices *Biomaterials* **23** 2737–50
- [153] Voskerician G *et al* 2003 Biocompatibility and biofouling of MEMS drug delivery devices *Biomaterials* **24** 1959–67
- [154] Valencia M *et al* 2011 Development of untethered SU-8 polymer scratch drive microrobots *2011 IEEE 24th Int. Conf. on Micro Electro Mechanical Systems* pp 1221–4
- [155] Zhu J *et al* 2012 Integrating process and novel sacrificial layer fabricating technique based on diluted SU-8 resist *Microelectron. Eng.* **93** 56–60
- [156] Chen Q *et al* 2011 Curved SU-8 structure fabrication based on the acid-diffusion effect *2011 IEEE 24th Int. Conf. on Micro Electro Mechanical Systems* pp 225–8
- [157] Zine-El-Abidine I and Okoniewski M 2009 A low-temperature SU-8 based wafer-level hermetic packaging for MEMS devices *IEEE Trans. Adv. Packaging* **32** 448–52
- [158] Kudryashov V *et al* 2003 Grey scale structures formation in SU-8 with e-beam and UV *Microelectron. Eng.* **67** 306–11
- [159] Cheng Y *et al* 1999 Wall profile of thick photoresist generated via contact printing *J. Microelectromech. Syst.* **8** 18–26
- [160] Chuang Y J *et al* 2003 A novel fabrication method of embedded micro-channels by using SU-8 thick-film photoresists *Sensors Actuators A* **103** 64–9
- [161] Mao X *et al* 2013 Two new methods to improve the lithography precision for SU-8 photoresist on glass substrate *J. Microelectromech. Syst.* **22** 124–30
- [162] Li N *et al* 2012 Non-planar surface bonding with spray-coated SU-8 as adhesive layer *Micro Nano Lett.* **7** 1220–2
- [163] Phatthanakun R *et al* 2008 Multi-step powder casting and x-ray lithography of SU-8 resist for complicated 3D microstructures *5th Int. Conf. on Electrical Engineering/Electronics, Computer, Telecommunications and Information Technology* pp 805–8
- [164] Ghantasala M K *et al* 2001 Patterning, electroplating and removal of SU-8 moulds by excimer laser micromachining *J. Micromech. Microeng.* **11** 133–9
- [165] Medina D *et al* 2012 Bonding, exposing and transferring technique in SU-8 and SU-8 laser micromachining combination for 3D, free-standing and multilevel microstructures *Micro Nano Lett.* **7** 412–4

- [166] Teh W *et al* 2005 Effect of low numerical-aperture femtosecond two-photon absorption on (SU-8) resist for ultrahigh-aspect-ratio microstereolithography *J. Appl. Phys.* **97** 054907
- [167] Wong W and Pun E 2001 Exposure characteristics and 3D profiling of SU8C resist using electron beam lithography *J. Vac. Sci. Technol. B* **19** 732–5
- [168] Tay F E H *et al* 2001 A novel micro-machining method for the fabrication of thick-film SU-8 embedded microchannels *J. Micromech. Microeng.* **11** 27–32
- [169] van Kan J A *et al* 2001 Proton beam micromachining: a new tool for precision 3D microstructures *Sensors Actuators A* **92** 370–4
- [170] Yu H *et al* 2004 Building embedded microchannels using a single layered SU-8, and determining Young's modulus using a laser acoustic technique *J. Micromech. Microeng.* **14** 1576–84
- [171] Kouba J *et al* 2007 SU-8: promising resist for advanced direct LIGA applications for high aspect ratio mechanical microparts *Microsyst. Technol.* **13** 311–7
- [172] Van Erps J *et al* 2013 Deep proton writing for the rapid prototyping of polymer micro-components for optical interconnects and optofluidics *Nucl. Instrum. Methods Phys. Res. B* **307** 243–7
- [173] Lorenz H *et al* 1998 High-aspect-ratio, ultrathick, negative-tone near-UV photoresist and its applications for MEMS *Sensors Actuators A* **64** 33–9
- [174] Yanagida H *et al* 2011 Simple removal technology using ozone solution for chemically-stable polymer used for MEMS *2011 IEEE 24th Int. Conf. on Micro Electro Mechanical Systems* pp 324–7
- [175] Yoshida S *et al* 2014 Development of UV-assisted ozone steam etching and investigation of its usability for SU-8 removal *J. Micromech. Microeng.* **24** 035007
- [176] Wagterveld R M *et al* 2006 Ultralow hysteresis superhydrophobic surfaces by excimer laser modification of SU-8 *Langmuir* **22** 10904–8
- [177] Melai J *et al* 2007 Considerations on using SU-8 as a construction material for high aspect ratio structures *10th Annual Workshop on Semiconductor Advances for Future Electronics and Sensors (SAFE) (Veldhoven, The Netherlands)* pp 529–534
- [178] Dellmann L *et al* 1998 Fabrication process of high aspect ratio elastic and SU-8 structures for piezoelectric motor applications *Sensors Actuators A* **70** 42–7
- [179] Seidemann V *et al* 2002 SU8-micromechanical structures with *in situ* fabricated movable parts *Microsyst. Technol.* **8** 348–50
- [180] Zou J *et al* 2004 A mould-and-transfer technology for fabricating scanning probe microscopy probes *J. Micromech. Microeng.* **14** 204–11
- [181] Truong T Q and Nguyen N T 2004 A polymeric piezoelectric micropump based on lamination technology *J. Micromech. Microeng.* **14** 632–8
- [182] Johansson A *et al* 2005 SU-8 cantilever sensor system with integrated readout *Sensors Actuators A* **123–24** 111–5
- [183] Song H-C *et al* 2003 Flexible low-voltage electro-optic polymer modulators *Appl. Phys. Lett.* **82** 4432–4
- [184] Nguyen N T *et al* 2004 Micro check valves for integration into polymeric microfluidic devices *J. Micromech. Microeng.* **14** 69–75
- [185] Nguyen N T *et al* 2004 A polymeric microgripper with integrated thermal actuators *J. Micromech. Microeng.* **14** 969–74
- [186] Luo C *et al* 2004 Releasing SU-8 structures using polystyrene as a sacrificial material *Sensors Actuators A* **114** 123–8
- [187] Kim B J *et al* 2001 A self-assembled monolayer-assisted surface microfabrication and release technique *Microelectron. Eng.* **57–8** 755–60
- [188] Cheng M C *et al* 2004 Dry release of polymer structures with anti-sticking layer *J. Vac. Sci. Technol. A* **22** 837–41
- [189] Haefliger D and Boisen A 2006 3D microfabrication in negative resist using printed masks *J. Micromech. Microeng.* **16** 951–7
- [190] Patel J N *et al* 2008 PDMS as a sacrificial substrate for SU-8-based biomedical and microfluidic applications *J. Micromech. Microeng.* **18** 095028
- [191] Ezkerra A *et al* 2007 Fabrication of SU-8 free-standing structures embedded in microchannels for microfluidic control *J. Micromech. Microeng.* **17** 2264
- [192] Peng Z C *et al* 2006 CMOS compatible integration of 3D microfluidic systems based on low-temperature transfer of SU-8 films *J. Microelectromech. Syst.* **15** 708–16
- [193] Chang J H-C *et al* 2012 Dry mechanical liftoff technology for metallization on parylene-C using SU-8 *2012 7th IEEE Int. Conf. on Nano/Micro Engineered and Molecular Systems* pp 286–9
- [194] Shirtcliffe N J *et al* 2004 The use of high aspect ratio photoresist (SU-8) for super-hydrophobic pattern prototyping *J. Micromech. Microeng.* **14** 1384
- [195] Kawai A *et al* 1994 Adhesion of photoresist pattern baked at 80 to 325° C to inorganic solid surface *Japan. J. Appl. Phys.* **33** L146
- [196] Carlier J *et al* 2004 Integrated microfluidics based on multi-layered SU-8 for mass spectrometry analysis *J. Micromech. Microeng.* **14** 619–24
- [197] Pan C T *et al* 2002 A low-temperature wafer bonding technique using patternable materials *J. Micromech. Microeng.* **12** 611–5
- [198] Walther F *et al* 2010 Surface hydrophilization of SU-8 by plasma and wet chemical processes *Surf. Interface Anal.* **42** 1735–44
- [199] Nordström M *et al* 2004 Rendering SU-8 hydrophilic to facilitate use in micro channel fabrication *J. Micromech. Microeng.* **14** 1614
- [200] Oruganti N *et al* 2013 Process variability in surface roughening of SU-8 by oxygen plasma *Microsyst. Technol.* **19** 971–8
- [201] Zhang J *et al* 2005 Argon plasma modification of SU-8 for very high aspect ratio and dense copper electroforming *J. Electrochem. Soc.* **152** C716–21
- [202] Nagaiyanallur V V *et al* 2014 Tailoring SU-8 Surfaces: covalent attachment of polymers by means of nitrene insertion *Langmuir* **30** 10107–11
- [203] Tseng F-G *et al* 2004 A surface-tension-driven fluidic network for precise enzyme batch-dispensing and glucose detection *Sensors Actuators A* **111** 107–17
- [204] Xue P *et al* 2014 Protein covalently conjugated SU-8 surface for the enhancement of mesenchymal stem cell adhesion and proliferation *Langmuir* **30** 3110–7
- [205] Tao S L *et al* 2008 Surface modification of SU-8 for enhanced biofunctionality and nonfouling properties *Langmuir* **24** 2631–6
- [206] Kim H-N *et al* 2011 Surface modification of 2D/3D SU-8 patterns with a swelling–deswelling method *Soft Matter* **7** 2989–93
- [207] Wang C *et al* 2005 A novel method for the fabrication of high-aspect ratio C-MEMS structures *J. Microelectromech. Syst.* **14** 348–58
- [208] Ceysens F and Puers R 2006 Creating multi-layered structures with freestanding parts in SU-8 *J. Micromech. Microeng.* **16** S19
- [209] Nazmov V *et al* 2015 Development and characterization of ultra high aspect ratio microstructures made by ultra deep x-ray lithography *J. Mater. Process. Technol.* **225** 170–7
- [210] Xiang Z *et al* 2013 Development of flexible neural probes using SU-8/parylene *The 8th Annual IEEE Int. Conf. on Nano/Micro Engineered and Molecular Systems*
- [211] Xue N *et al* 2012 A SU-8-based microfabricated implantable inductively coupled passive RF wireless intraocular pressure sensor *Microelectromech. J. Syst.* **21** 1338–46

- [212] Lucibello A *et al* 2013 RF MEMS switches fabrication by using SU-8 technology *Microsyst. Technol.* **19** 929–36
- [213] Song Y J *et al* 2004 Fabrication of an SU-8 based microfluidic reactor on a PEEK substrate sealed by a ‘flexible semi-solid transfer’ (FST) process *J. Micromech. Microeng.* **14** 932–40
- [214] Conedera V *et al* 2007 Surface micromachining technology with two SU-8 structural layers and sol-gel, SU-8 or SiO₂/sol-gel sacrificial layers *J. Micromech. Microeng.* **17** N52–7
- [215] Bao X *et al* 2011 Design and fabrication of insect-inspired composite wings for MAV application using MEMS technology *J. Micromech. Microeng.* **21** 125020
- [216] Mastrangeli M *et al* 2014 Liquid-filled sealed MEMS capsules fabricated by fluidic self-assembly 2014 *IEEE 27th Int. Conf. on Micro Electro Mechanical Systems* pp 56–59
- [217] Barth P W *et al* 1985 Flexible circuit and sensor arrays fabricated by monolithic silicon technology *IEEE Trans. Electron Devices* **32** 1202–5
- [218] Pedersen M *et al* 1998 High-performance condenser microphone with fully integrated CMOS amplifier and DC-DC voltage converter *J. Microelectromech. Syst.* **7** 387–94
- [219] Sato K *et al* 1973 Novel planar multilevel interconnection technology utilizing polyimide *IEEE Trans. Parts Hybrids Packaging* **PH9** 176–80
- [220] Mukai K *et al* 1978 Planar multilevel interconnection technology employing a polyimide *IEEE J. Solid-State Circuits* **13** 462–7
- [221] Wilson A M 1981 Polyimide insulators for multilevel interconnections *Thin Solid Films* **83** 145–63
- [222] Sasaki S *et al* 1989 A new multichip module using a copper polyimide multilayer substrate *IEEE Trans. Compon. Hybrids Manuf. Technol.* **12** 658–62
- [223] Tsumita N *et al* 1981 Fabrication of x-ray masks using anisotropic etching of (1 1 0) Si and shadowing techniques *J. Vac. Sci. Technol.* **19** 1211–3
- [224] Shamma-Donoghue S A *et al* 1982 Thin-film multielectrode arrays for a cochlear prosthesis *IEEE Trans. Electron Devices* **29** 136–44
- [225] White R L *et al* 1983 Thin-film electrodes for an artificial ear *J. Vac. Sci. Technol.* **1** 287–95
- [226] Kim Y J and Allen M G 1999 *In situ* measurement of mechanical properties of polyimide films using micromachined resonant string structures *IEEE Trans. Compon. Packaging Technol.* **22** 282–90
- [227] Frazier A B and Allen M G 1993 Piezoresistive graphite polyimide thin-films for micromachining applications *J. Appl. Phys.* **73** 4428–33
- [228] Kim J S *et al* 2008 A locally cured polyimide-based humidity sensor with high sensitivity and high speed *IEEE Sensors 2008* pp 434–7
- [229] Lake J H *et al* 2011 Maskless grayscale lithography using a positive-tone photodefinable polyimide for MEMS applications *J. Microelectromech. Syst.* **20** 1483–8
- [230] Wang Z *et al* 2011 Fabrication of fluorinated polyimide optical waveguides by microopen direct writing technology *Opt. Lasers Eng.* **49** 880–4
- [231] Memmi D *et al* 2002 Fabrication of capacitive micromechanical ultrasonic transducers by low-temperature process *Sensors Actuators A* **99** 85–91
- [232] Eray M *et al* 1994 Highly stable bilayer-lipid membranes (blms) formed on microfabricated polyimide apertures *Biosens. Bioelectron.* **9** 343–51
- [233] Minami K *et al* 1999 A bellows-shape electrostatic microactuator *Sensors Actuators A* **72** 269–76
- [234] Schmidt M A *et al* 1988 Design and calibration of a microfabricated floating-element shear-stress sensor *IEEE Trans. Electron Devices* **35** 750–7
- [235] Ahn C H *et al* 1994 A fully integrated planar toroidal inductor with a micromachined nickel iron magnetic bar *IEEE Trans. Compon. Packag. Manuf. Technol.* **A** **17** 463–9
- [236] Suh J W *et al* 1997 Organic thermal and electrostatic ciliary microactuator array for object manipulation *Sensors Actuators A* **58** 51–60
- [237] Pakula L S *et al* 2004 Fabrication of a CMOS compatible pressure sensor for harsh environments *J. Micromech. Microeng.* **14** 1478–83
- [238] Kim S H *et al* 2005 Effect of surface roughness on the adhesion properties of Cu/Cr films on polyimide substrate treated by inductively coupled oxygen plasma *Surf. Coat. Technol.* **200** 2072–9
- [239] Liu Y *et al* 2011 Plasma-induced damages to polyimide diaphragms during Si dry-etching in micropump fabrication processes *J. Photopolym. Sci. Technol.* **24** 293–8
- [240] Jurgensen C W and Shaqfeh E S G 1989 Factors controlling the etching rate and etching profile in the O-2 reactive ion etching pattern transfer step in multilevel lithography *Polym. Eng. Sci.* **29** 878–81
- [241] Singh J K *et al* 1987 Dependence of process parameters on planarization isolation and etching of sloped vias in polyimides for gaas ics *Proc. IEEE* **75** 850–2
- [242] Egitto F D *et al* 1985 Plasma-etching of organic materials 1. Polyimide in O₂-CF₄ *J. Vac. Sci. Technol. B* **3** 893–904
- [243] Turban G and Rapeaux M 1983 Dry etching of polyimide in O₂-CF₄ and O₂-Sf₆ Plasmas *J. Electrochem. Soc.* **130** 2231–6
- [244] Juan W H and Pang S W 1994 High-aspect-ratio polyimide etching using an oxygen plasma generated by electron-cyclotron-resonance source *J. Vac. Sci. Technol. B* **12** 422–6
- [245] Buder U *et al* 2006 Reactive ion etching for bulk structuring of polyimide *Sensors Actuators A* **132** 393–9
- [246] Guo H *et al* 2015 Localized etching of polymer films using an atmospheric pressure air microplasma jet *J. Micromech. Microeng.* **25** 015010
- [247] Pethig R *et al* 1998 Development of biofactory-on-a-chip technology using excimer laser micromachining *J. Micromech. Microeng.* **8** 57–63
- [248] Martin P M *et al* 1999 Laminated plastic microfluidic components for biological and chemical systems *J. Vac. Sci. Technol. A* **17** 2264–9
- [249] Pan C T 2004 Perpendicular magnetic anisotropic field for polyimide-based microactuator with excimer laser ablation *Sensors Actuators A* **113** 240–7
- [250] Lin K L and Jain K 2009 Design and fabrication of stretchable multilayer self-aligned interconnects for flexible electronics and large-area sensor arrays using excimer laser photoablation *IEEE Electron Device Lett.* **30** 14–7
- [251] Zhao Y *et al* 2013 A simple and quick fabrication method of microfluidic cell sorter using Dielectrophoresis 2013 *IEEE 7th Int. Conf. on Nano/Molecular Medicine and Engineering* pp 32–35
- [252] Dyer P E 2003 Excimer laser polymer ablation: twenty years on *Appl. Phys. A* **77** 167–73
- [253] Schwarz A *et al* 1998 Micropatterning of biomolecules on polymer substrates *Langmuir* **14** 5526–31
- [254] Engel J *et al* 2003 Development of polyimide flexible tactile sensor skin *J. Micromech. Microeng.* **13** 359–66
- [255] Pedersen M *et al* 1997 A silicon condenser microphone with polyimide diaphragm and backplate *Sensors Actuators A* **63** 97–104

- [256] Pedersen M *et al* 1997 An IC-compatible polyimide pressure sensor with capacitive readout *Sensors Actuators A* **63** 163–8
- [257] Metz S *et al* 2004 Polyimide and SU-8 microfluidic devices manufactured by heat-depolymerizable sacrificial material technique *Lab Chip* **4** 114–20
- [258] Li M H *et al* 2001 Surface micromachined polyimide scanning thermocouple probes *J. Microelectromech. Syst.* **10** 3–9
- [259] McNamara S *et al* 2005 Ultracompliant thermal probe array for scanning non-planar surfaces without force feedback *J. Micromech. Microeng.* **15** 237–43
- [260] Bayrashev A and Ziaie B 2003 Silicon wafer bonding through RF dielectric heating *Sensors Actuators A* **103** 16–22
- [261] Itabashi T and Zussman M P 2010 High temperature resistant bonding solutions enabling thin wafer processing (characterization of polyimide base temporary bonding adhesive for thinned wafer handling) *2010 Proc. 60th Electronic Components and Technology Conf.* pp 1877–880
- [262] Azad J B *et al* 2013 Release of MEMS devices with hard-baked polyimide sacrificial layer *Proc. SPIE Advanced Lithography* pp 868226
- [263] Nayve R *et al* 2004 High-resolution long-array thermal ink jet printhead fabricated by anisotropic wet etching and deep Si RIE *J. Microelectromech. Syst.* **13** 814–21
- [264] Lubecke V M *et al* 2007 Polyimide spacers for flip-chip optical MEMS *J. Microelectromech. Syst.* **16** 959–68
- [265] Ordóñez J S *et al* 2013 Silicone rubber and thin-film polyimide for hybrid neural interfaces—a MEMS-based adhesion promotion technique *2013 6th Int. IEEE/EMBS Conf. on Neural Engineering* pp 872–5
- [266] Thuau D *et al* 2013 Stress relaxation of polyimide (PI) cantilevers using low energy ion bombardment *Soft Mater.* **11** 414–20
- [267] Lindeberg M and Hjort K 2009 High aspect ratio multiple wire microvias in flexible PCBs *Circuit World* **35** 18–21
- [268] Zha J-W *et al* 2013 Fabrication and properties of high performance polyimide nanofibrous films by electrospinning *2013 IEEE Int. Conf. on Solid Dielectrics* pp 923–6
- [269] Pedersen M *et al* 1998 Development and fabrication of capacitive sensors in polyimide *Sensors Mater.* **10** 1–20
- [270] Márton G *et al* 2015 A polymer-based spiky microelectrode array for electrocorticography *Microsyst. Technol.* **21** 619–24
- [271] Nakamura Y *et al* 1996 Effect of oxygen plasma etching on adhesion between polyimide films and metal *Thin Solid Films* **291** 367–9
- [272] Ebefors T *et al* 1998 New small radius joints based on thermal shrinkage of polyimide in V-grooves for robust self-assembly 3D microstructures *J. Micromech. Microeng.* **8** 188–94
- [273] Ebefors T *et al* 1998 Dynamic actuation of polyimide V-groove joints by electrical heating *Sensors Actuators A* **67** 199–204
- [274] Novak J L and Wheeler B C 1986 Recording from the aplysia abdominal-ganglion with a planar microelectrode array *IEEE Trans. Biomed. Eng.* **33** 196–202
- [275] Campbell P K *et al* 1991 A silicon-based, 3D neural interface—manufacturing processes for an intracortical electrode array *IEEE Trans. Biomed. Eng.* **38** 758–68
- [276] Metz S *et al* 2004 Polyimide microfluidic devices with integrated nanoporous filtration areas manufactured by micromachining and ion track technology *J. Micromech. Microeng.* **14** 324–31
- [277] Kim S H *et al* 2005 Texture classification using a polymer-based MEMS tactile sensor *J. Micromech. Microeng.* **15** 912–20
- [278] Dayeh S A *et al* 2005 Micromachined infrared bolometers on flexible polyimide substrates *Sensors Actuators A* **118** 49–56
- [279] Mahmood A *et al* 2006 Micromachined bolometers on polyimide *Sensors Actuators A* **132** 452–9
- [280] Ahmed M *et al* 2012 MEMS sensors on flexible substrates towards a smart skin *2012 IEEE Sensors* pp 1–4
- [281] Bratten C D T *et al* 1997 Micromachining sensors for electrochemical measurement in subnanoliter volumes *Anal. Chem.* **69** 253–8
- [282] Cai X X *et al* 2000 Miniaturized electroanalytical sensor systems in micromachined structures *Electroanalysis* **12** 631–9
- [283] Hediger S *et al* 1999 Fabrication of a novel microsystem for the electrical characterisation of cell arrays *Sensors Actuators B* **56** 175–80
- [284] Liu Y *et al* 2011 Planar diffuser/nozzle micropumps with extremely thin polyimide diaphragms *Sensors Actuators A* **169** 259–65
- [285] Gowrishetty U R *et al* 2010 Fabrication of polyimide bi-stable diaphragms using oxide compressive stresses for the field of ‘Buckle MEMS’ *J. Micromech. Microeng.* **20** 075013
- [286] Huang I-Y *et al* 2010 Lifting angle of polyimide self-assembly surface-micromachined structure *J. Micro Nanolithogr. MEMS MOEMS* **9** 023006
- [287] Jeon M *et al* 2014 Partially flexible MEMS neural probe composed of polyimide and sucrose gel for reducing brain damage during and after implantation *J. Micromech. Microeng.* **24** 025010
- [288] Szwarc M 1947 Some remarks on the $\text{CH}_2 = \text{benzene} = \text{CH}_2$ molecule *Discuss. Faraday Soc.* **2** 46–9
- [289] Gorham W F 1966 A new, general synthetic method for the preparation of linear poly-p-xylylenes *J. Polym. Sci. A* **4** 3027–39
- [290] Fortin J B and Lu T-M 2004 Deposition kinetics for polymerization via the Gorham route *Chemical Vapor Deposition Polymerization* (New York: Springer) pp 41–55
- [291] Yeh Y S *et al* 1990 Polymerization of para-xylylene derivatives. VI. Morphology of parylene N and parylene C films investigated by gas transport characteristics *J. Polym. Sci. B* **28** 545–68
- [292] Hsu J-M *et al* 2008 Effect of thermal and deposition processes on surface morphology, crystallinity, and adhesion of Parylene-C *Sensors Mater.* **20** 071–86
- [293] Rui Y *et al* 2011 Parylene-based implantable Pt-black coated flexible 3-D hemispherical microelectrode arrays for improved neural interfaces *Microsyst. Technol.* **17** 437–42
- [294] Huang R and Tai Y 2009 Parylene-pocket chip integration *IEEE 22nd Int. Conf. on Micro Electro Mechanical Systems 2009* pp 749–52
- [295] Kurihara M *et al* 2012 3d laser lithography combined with parylene coating for the rapid fabrication of 3d microstructures *2012 IEEE 25th Int. Conf. on Micro Electro Mechanical Systems* pp 196–9
- [296] Charmet J *et al* 2010 Solid on liquid deposition *Thin Solid Films* **518** 5061–5
- [297] Komatsu S *et al* 2009 Peristaltic micropump fabricated by depositing parylene directly on liquid *Int. Solid-State Sensors Actuators and Microsystems Conf. 2009. TRANSDUCERS 2009* pp 2007–10
- [298] Prihandana G S *et al* 2012 Polyethersulfone membrane coated with nanoporous Parylene for ultrafiltration *J. Microelectromech. Syst.* **21** 1288–90

- [299] Demirel G *et al* 2010 Template-based and template-free preparation of nanostructured parylene via oblique angle polymerization *Thin Solid Films* **518** 4252–5
- [300] von Metzen R P *et al* 2011 Diffusion-limited deposition of Parylene C *J. Microelectromech. Syst.* **20** 239–50
- [301] Charlson E M *et al* 1992 Temperature selective deposition of Parylene-C *IEEE Trans. Biomed. Eng.* **39** 202–6
- [302] Xu Y and Tai Y-C 2003 Selective deposition of parylene C for underwater shear-stress sensors *12th Int. Conf. on TRANSDUCERS Solid-State Sensors Actuators and Microsystems* pp 1307–10
- [303] Kramer P *et al* 1984 Polymerization of Para-xylylene derivatives (parylene polymerization) 1. Deposition kinetics for Parylene-N and Parylene-C *J. Polym. Sci. Polym. Chem. Ed.* **22** 475–91
- [304] Gazicki M *et al* 1985 Polymerization of para-xylylene derivatives (parylene polymerization) 2. Heat-effects during deposition of parylene-C at different temperatures *J. Polym. Sci. A* **23** 2255–77
- [305] Vaeth K M and Jensen K F 2000 Transition metals for selective chemical vapor deposition of parylene-based polymers *Chem. Mater.* **12** 1305–13
- [306] Hassler C *et al* 2010 Characterization of Parylene C as an encapsulation material for implanted neural prostheses *J. Biomed. Mater. Res. B Appl. Biomater.* **93B** 266–74
- [307] Specialty Coating Systems 2001 Specialty Coating Systems: Solvent Resistance of Parylene
- [308] Ratier B *et al* 1999 Vapor deposition polymerization and reactive ion beam etching of poly(p-xylylene) films for waveguide applications *Opt. Mater.* **12** 229–33
- [309] Majid N *et al* 1989 The parylene-aluminum multilayer interconnection system for wafer scale integration and wafer scale hybrid packaging *J. Electron. Mater.* **18** 301–11
- [310] Yeh J T C and Grebe K R 1983 Patterning of poly-paraxylylenes by reactive ion etching *J. Vac. Sci. Technol. A* **1** 604–8
- [311] Standaert T *et al* 2001 High-density plasma patterning of low dielectric constant polymers: a comparison between polytetrafluoroethylene, parylene-N, and poly(arylene ether) *J. Vac. Sci. Technol. A* **19** 435–46
- [312] Loeb G E *et al* 1995 Toward the ultimate metal microelectrode *J. Neurosci. Methods* **63** 175–83
- [313] Schmidt E M *et al* 1995 Laser exposure of Parylene-C insulated microelectrodes, *J. Neurosci. Methods* **62** 89–92
- [314] Weiland J D *et al* 1997 Recessed electrodes formed by laser ablation of parylene coated, micromachined silicon probes *Proc. of the 19th Annual Int. Conf. of the IEEE Engineering in Medicine and Biology Society 1997* vol. 5 pp 2273–6
- [315] Liu Y *et al* 2013 Parylene origami structure for intraocular implantation *The 17th Int. Conf. on Solid-State Sensors Actuators and Microsystems (TRANSDUCERS & EUROSENSORS XXVII)* pp 1549–52
- [316] Park J *et al* 2013 Flexible neurocage array for live neural network study *2013 IEEE 26th Int. Conf. on Micro Electro Mechanical Systems* pp 295–8
- [317] Chou N and Kim S 2013 A fabrication method of out-of-plane stretchable and flexible electrodes based on PDMS *Proc. SPIE Micro + Nano Materials, Devices, and Applications* pp 89233Q
- [318] Crum B and Li W 2013 Parylene-based fold-and-bond wireless pressure sensor *2013 8th IEEE Int. Conf. on Nano/Micro Engineered and Molecular Systems* pp 1155–8
- [319] Yu H *et al* 2012 Fabrication of electroplated nickel multielectrode microprobes with flexible parylene cable *2012 IEEE 25th Int. Conf. on Micro Electro Mechanical Systems* pp 239–42
- [320] Yamagiwa S *et al* 2013 Self-curling and-sticking flexible substrate for ECoG electrode array *2013 IEEE 26th Int. Conf. on Micro Electro Mechanical Systems* pp 480–3
- [321] Noh H S *et al* 2004 Wafer bonding using microwave heating of parylene intermediate layers *J. Micromech. Microeng.* **14** 625
- [322] Kim H and Najafi K 2005 Characterization of low-temperature wafer bonding using thin-film parylene *J. Microelectromech. Syst.* **14** 1347–55
- [323] Shu Q *et al* 2008 Wafer bonding with intermediate parylene layer *9th International Conference on Solid-State and Integrated-Circuit Technology 2008* pp 2428–31
- [324] Lee J H *et al* 2004 Microstructure and adhesion of Au deposited on parylene-c substrate with surface modification for potential immunoassay application *IEEE Trans. Plasma Sci.* **32** 505–9
- [325] Sharma A K and Yasuda H 1982 Effect of glow discharge treatment of substrates on parylene-substrate adhesion *J. Vac. Sci. Technol.* **21** 994–8
- [326] Rezai P *et al* 2011 Plasma enhanced bonding of polydimethylsiloxane (PDMS) with parylene *2011 16th Int. Solid-State Sensors Actuators and Microsystems Conference (TRANSDUCERS)* pp 1340–3
- [327] Trantidou T *et al* 2012 Oxygen plasma induced hydrophilicity of Parylene-C thin films *Appl. Surf. Sci.* **261** 43–51
- [328] Bi X *et al* 2014 Super Hydrophobic Parylene-C produced by consecutive O₂ and SF₆ plasma treatment *J. Microelectromech. Syst.* **23** 628–35
- [329] Delivopoulos E *et al* 2009 Guided growth of neurons and glia using microfabricated patterns of parylene-C on a SiO₂ background *Biomaterials* **30** 2048–58
- [330] Wahjudi P N *et al* 2009 Improvement of metal and tissue adhesion on surface-modified parylene C *J. Biomed. Mater. Res. A* **89** 206–14
- [331] Li W *et al* 2010 Wafer-level parylene packaging with integrated RF electronics for wireless retinal prostheses *J. Microelectromech. Syst.* **19** 735–42
- [332] Kuo H-I *et al* 2010 Development of micropackage technology for biomedical implantable microdevices using parylene C as water vapor barrier coatings *2010 IEEE Sensors* pp 438–41
- [333] Chang J H *et al* 2011 Adhesion-enhancing surface treatments for parylene deposition *2011 16th Int. Solid-State Sensors Actuators and Microsystems Conf. (TRANSDUCERS)* pp 390–3
- [334] Kang D *et al* 2012 *In situ* heating to improve adhesion for parylene-on-parylene deposition *2012 7th IEEE Int. Conf. on Nano/Micro Engineered and Molecular Systems* pp 226–9
- [335] Nandra M S *et al* 2011 A Parylene-based microelectrode array implant for spinal cord stimulation in rats *2011 IEEE 24th Int. Conf. on Micro Electro Mechanical Systems* pp 1007–10
- [336] Lu B *et al* 2011 Ultrathin parylene-C semipermeable membranes for biomedical applications *2011 IEEE 24th Int. Conf. on Micro Electro Mechanical Systems* pp 505–8
- [337] Li P-Y *et al* 2010 A parylene bellows electrochemical actuator *J. Microelectromech. Syst.* **19** 215–28
- [338] Gensler H *et al* 2011 Rapid non-lithography based fabrication process and characterization of Parylene C bellows for applications in MEMS electrochemical actuators *2011 16th Int. Solid-State Sensors Actuators and Microsystems Conf. (TRANSDUCERS)* pp 2347–50
- [339] Gensler H *et al* 2012 An implantable MEMS micropump system for drug delivery in small animals *Biomed. Microdevices* **14** 483–96

- [340] Byun D *et al* 2013 Fabrication of a flexible penetrating microelectrode array for use on curved surfaces of neural tissues *J. Micromech. Microeng.* **23** 125010
- [341] Kim E G *et al* 2014 A hybrid silicon–parylene neural probe with locally flexible regions *Sensors Actuators B* **195** 416–22
- [342] Seymour J P *et al* 2011 Novel multi-sided, microelectrode arrays for implantable neural applications *Biomed. Microdevices* **13** 441–51
- [343] Sun X *et al* 2012 Design and fabrication of flexible parylene-based inductors with electroplated NiFe magnetic core for wireless power transmission system *2012 7th IEEE Int. Conf. on Nano/Micro Engineered and Molecular Systems* pp 238–42
- [344] Ledochowitsch P *et al* 2011 Fabrication and testing of a large area, high density, parylene MEMS μ ECoG array *2011 IEEE 24th Int. Conf. on Micro Electro Mechanical Systems* pp 1031–4
- [345] Lei-Chun C *et al* 2014 A parylene-C based 16 channels flexible bio-electrode for ECoG recording *2014 IEEE Sensors* pp 877–80
- [346] Gutierrez C A and Meng E 2011 A subnanowatt microbubble pressure sensor based on electrochemical impedance transduction in a flexible all-parylene package *2011 IEEE 24th Int. Conf. on Micro Electro Mechanical Systems* pp 549–52
- [347] Yu L and Meng E 2014 A microbubble pressure transducer with bubble nucleation core *2014 IEEE 27th Int. Conf. on Micro Electro Mechanical Systems* pp 104–7